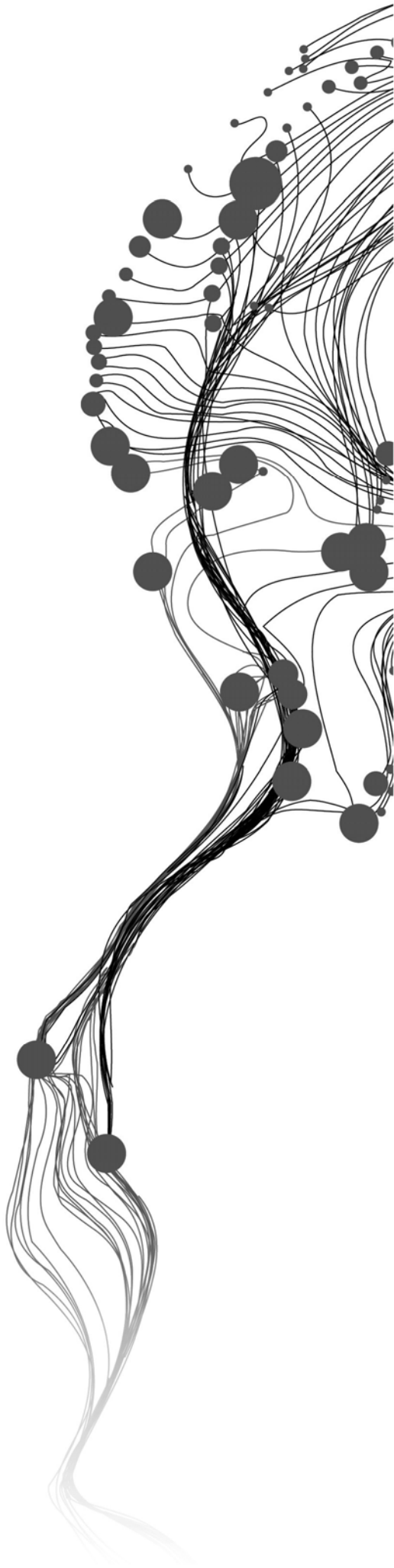


APPLICATION OF THE TOR VERGATA SCATTERING MODEL FOR SIMULATING L-BAND BACKSCATTERING DURING THE CORN GROWTH CYCLE

RASHA ELKHESHIEN
February, 2011

SUPERVISORS:
Dr., R., Van der Velde
Ir, W.J., Timmermans



APPLICATION OF THE TOR VERGATA SCATTERING MODEL FOR SIMULATING L-BAND BACKSCATTERING DURING THE CORN GROWTH CYCLE

RASHA ELKHESHIEN

Enschede, The Netherlands, February, 2011

Thesis submitted to the Faculty of Geo-Information Science and Earth Observation of the University of Twente in partial fulfilment of the requirements for the degree of Master of Science in Geo-information Science and Earth Observation.

Specialization: Water Resources and Environmental Management

SUPERVISORS:

Dr., R., Van der Velde

Ir, W.J., Timmermans

THESIS ASSESSMENT BOARD:

Prof.Dr, Z., Bob Su (Chairman)

Prof. Dr. Ir., N.C., van de Giesen (External Examiner, Faculty of Civil Engineering and Geosciences - Delft University)

DISCLAIMER

This document describes work undertaken as part of a programme of study at the Faculty of Geo-Information Science and Earth Observation of the University of Twente. All views and opinions expressed therein remain the sole responsibility of the author, and do not necessarily represent those of the Faculty.

ABSTRACT

The presence of vegetation complicates the retrieval of soil moisture from microwave remote sensing. Canopies contribute to total amount scattering and attenuate soil surface scattering, which reduces the sensitivity of microwave observations to soil moisture. On the other hand, microwave scattering along soil-vegetation pathways may enhance the soil moisture sensitivity of microwave observations. Most recently, detailed crop backscattering models have been developed to investigate the sensitivity of microwave observations to the land surface properties, such as soil moisture, theoretically. Interpretation of microwave response is a complex task, since it is affected by many parameters. Apart from soil moisture, also the soil roughness, plant moisture content and morphology (i.e., shape, dimensions, orientation, and relative location of vegetation elements) play an important role in the backscatter simulations.

For this research the discrete medium scattering model developed by the Tor Vergata University (Rome, Italy) has been applied to simulate the L-band (1.6 GHz) backscattering from a corn field throughout a growth cycle. This model, hereafter referred to as the Tor Vergata model, is based on radiative transfer theory and solves the relevant equations via the matrix doubling algorithm, which includes multiple scattering effects. The model simulations are compared against measurements by the NASA-George Washington University truck mounted scatterometer collected throughout a corn growth cycle.

This thesis contributes towards the development of the Tor Vergata modelling system by including recently proposed dielectric mixing models and evaluating a new version of the Tor Vergata model that considers partially covered canopies. A satisfactory agreement is observed between simulated and measured backscattering when fraction vegetation cover is included. At HH polarization, however, a systematic backscatter overestimation remains. Part of the overestimations is resolved by including the more recently developed dielectric mixing models and varying the stem inclination angle over a broader range. However, also the field measured vegetation morphology may include uncertainties.

ACKNOWLEDGEMENTS

*“To him belong all that is in the heavens and all that on the earth, and all that in between them,
and all that is under the soil “* *Surat Ta-Ha—Aya (6)*

I owe my deepest gratitude to the Egyptian revolution on 25th January 2011 and its blessed martyrs that inspired me to continue working through hard times

First, I am heartily thankful to my supervisor, Rogier van der Velde. This thesis would not have been possible unless his encouragement, guidance and support from the initial to the final stage that enabled me to develop and understand this research.

Secondly, special thanks go to P.Ferrazzoli from Tor Vergata University in Rome, Italy for providing the Tor Vergata scattering model and his support through this research. Also, I am thankful to USDA-ARS (United States Department of Agriculture-Agricultural Research Service) for providing the dataset used for carrying out this research.

Finally, I am indebted to many of my colleagues to support me especially, Jowan Khorsheed, Sania Rahman and Ahmad Fallatah. I offer my regards and blessings to my family who supported me in any respect during the completion of this research.

Rasha Elkheshien

TABLE OF CONTENTS

1.	Introduction.....	1
1.1.	Background.....	1
1.2.	Thesis contribution.....	2
1.3.	Problem definition.....	2
1.4.	Research objective and questions.....	2
1.5.	Thesis outline.....	3
2.	Material.....	5
2.1.	Study area description.....	5
2.2.	Data sets.....	5
3.	Background.....	10
3.1.	Introduction.....	10
3.2.	Scatterers representation.....	11
3.3.	Dielectric models.....	11
4.	Tor Vergata model.....	13
4.1.	Geometric representation.....	13
4.2.	Dielectric representation.....	13
4.3.	Integrating the effect of different scatterers.....	14
4.4.	Backscatter calculation over closed canopies.....	16
4.5.	Backscatter calculation over open canopies.....	17
5.	Application of Tor Vergata model.....	18
6.	Backscatter simulation.....	20
6.1.	Effects of dielectric models.....	20
6.2.	Vegetation geometry effects.....	23
6.3.	Effect of fraction vegetation cover.....	28
7.	Comparing the scattering components.....	30
7.1.	Surface scattering.....	31
7.2.	Vegetation scattering.....	32
7.3.	Vegetation-Surface scattering.....	33
8.	Summary and Conclusions.....	34

LIST OF FIGURES

Figure (2-1) Location of OPE ³ study area	5
Figure (2-2) The truck mounted radar/radiometer system called ComRad	6
Figure (2-3) Schematization of the experimental setup during 2002 OPE ³ field campaign.....	6
Figure (2-4) Moisture content for corn leaves and stems	7
Figure (2-5) Corn geometrical parameters	7
Figure (2-6) Stalk geometry values through the OPE ³ campaign.....	8
Figure (2-7) leaf geometrical parameters	8
Figure (2-8) The 2-m grid board placed in soil surface for characterization of surface roughness	9
Figure (2-9) soil moisture measured in field	9
Figure (3-1) Backscattering process over vegetated covered surface affecting active microwave observations	10
Figure (4-1) Corn Canopy model (Della Vecchia, et al., 2006)	13
Figure (4-2) Scattering mechanism in the matrix doubling algorithm (Bracaglia, et al., 1995)	14
Figure (4-3) Scattering and transmission matrices for downward (left) and upward (right) travelling radiation(Eom & Fung, 1984)	15
Figure (4-4) Scattering process for unit incident intensity	16
Figure (6-1) Backscatter simulations with measured ones using four dielectric model combinations	21
Figure (6-2) measured vs. simulated backscattering for Dobson soil model together with Ulaby & El-Rayes and Matzler vegetation models	21
Figure (6-3) measured vs. simulated backscattering for Mironov soil model together with Ulaby & El-Rayes and Matzler vegetation models	22
Figure (6-4) Effect of different leaf orientation on Tor Vergata Model	25
Figure (6-5) Effect of stem orientation on simulated backscattering	27
Figure (6-6) Effect of FVC on Tor Vergata model	29
Figure (7-1) Surface scattering component	31
Figure (7-2) Vegetation scattering component	32
Figure (7-3) Vegetation-Surface scattering.....	33

LIST OF TABLES

Table (5-1) Inputs for TorVergata model.....	18
Table (6-1) Average values for statistical measures comparing measured and simulated backscattering for different soil and vegetation dielectric models.....	23
Table (6-2) Average values for statistical measures comparing measured and simulated backscattering for HH and VV polarization	23
Table (6-3) statistical measures showing sensitivity of Tor Vergata model towards effect of different leaf orientations	25
Table (6-4) Several Statistical measures to compare measured and simulated σ_0 at different maximum stem angles	27
Table (6-5) Several Statistical measures to compare measured and simulated σ_0 at HH & VV polarization.	27
Table (6-6) statistical measures showing the differences between including FVC and the previous version of Tor Vergata model	28

1. INTRODUCTION

1.1. Background

Water and energy fluxes at the earth surface are strongly dependent upon soil moisture. Soil moisture constrains the partitioning of solar radiation into sensible and latent heat and drives the infiltration and the production of runoff. However, spatially variable rainfall, soil properties, topography and land cover causes soil moisture typically to be highly variable in both space and time (Famiglietti, Rudnicki, & Rodell, 1998). This variability should be taken into account in hydrological and climate models (Schmugge, Kustas, Ritchie, Jackson, & Rango, 2002; Wood et al., 1993).

Microwave remote sensing provides a unique ability to monitor soil moisture at spatial and temporal scales that is needed to meet the requirements of various applications (Narayan, Lakshmi, & Njoku, 2004). Microwave measurements have shown to be sensitive to changes in soil moisture (Rajat Bindlish et al., 2003; Narayan, et al., 2004; Njoku et al., 2002; Owe, de Jeu, & Walker, 2001; Wen, Su, & Ma, 2003).

As a result, European Space Agency (ESA) launched the Soil Moisture and Oceanic Salinity (SMOS) mission in November 2009 (Kerr et al., 2010; 2001). This satellite carries the first polar-orbiting spaceborne 2-D interferometric radiometer, which enables the measurements of L-band brightness temperatures at 50 km spatial resolution. Similarly NASA is in preparation of a soil moisture mission, which is called the Soil Moisture Active and Passive (SMAP) mission. SMAP will include both active and passive L-Band sensors and is scheduled for launch in 2015 (Entekhabi, Njoku, & O'Neill, 2009). The same combined active/microwave microwave setup will be used for mapping the ocean salinity by Aquarius mission (Vine, Pellerano, Lagerloef, Yueh, & Colomb, 2006), details about the operational satellites of microwave remote sensing and different methods applied for soil moisture retrieval was reviewed by Wagner et al. (2007).

There are soil moisture products available from both active and passive microwave sensors separately. Most recently, combined passive/active microwave retrieval algorithm have been proposed (R. Bindlish & Barros, 2002; Chauhan, 1997; Chauhan, Le Vine, & Lang, 1994; Njoku, Wilson, Yueh, & Rahmat-Samii, 2000; Wigneron, Ferrazzoli, Calvet, & Bertuzzi, 1999; Wilson et al., 2001). However, the advantages offered by a synergistic use of radar and radiometric instruments are not yet fully exploited in retrieval algorithms (Wigneron, et al., 1999). So, having a single model that can simulate both active and passive measurements is an important step in understanding how both active and passive microwave can provide complementary information to be used for retrieving soil moisture (Chauhan, et al., 1994; Njoku, et al., 2000; Wilson, et al., 2001).

The presence of vegetation complicates the retrieval of soil moisture. Canopies contribute to total amount scattering and attenuate soil surface scattering, which reduces the sensitivity of microwave observations to soil moisture (Schmugge, 1983; F. Ulaby & Batlivala, 1976). On the other hand, microwave scattering along soil-vegetation pathways may enhance the soil moisture sensitivity of microwave observations. Detailed crop backscattering models have been developed to investigate the sensitivity of microwave observations to the land surface properties, such as soil moisture, theoretically (Cookmartin et al., 2000; Della Vecchia et al., 2008; Macelloni, Paloscia, Pampaloni, Marliani, & Gai, 2001; Maity, Patnaik, Chakraborty, & Panigrahy, 2004; F. Ulaby, 1980; F. Ulaby & Bush, 1976). Interpretation of microwave

response is a complex task, since it is affected by many parameters. Apart from soil moisture, also the soil roughness, plant moisture content, and morphology (i.e., shape, dimensions, orientation, and relative location of vegetation elements) play an important role in the backscatter simulations. However, important advances have been achieved, both in the electromagnetic characterization of single scatterers and in the combination of contributions.

Physically based vegetation models adopt the discrete medium approach which represents the canopy as set of discrete dielectric scatterers. Vegetation elements are described as dielectric bodies with simplified shapes. It permits to investigate the electromagnetic interaction among all vegetation components through combining vegetation and soil scattering theories and using input variables that can be measured directly in the fields.

Several models have been developed to simulate both passive and active microwave observations based on absorption and scattering cross sections defined by the scatterers. For example, Attema and Ulaby (1978) modelled vegetation as a water cloud to derive backscattering coefficient. Afterwards, Lang and Sidhu (1983) developed the turbid medium approach for calculating microwave scattering and emission based on wave theory. On the other hand, Ulaby et al. (1988) adopted a first order radiative transfer method for calculating the microwave signatures (MIMICS) modified by Toure et al. (1994) for crops whereas Karam et al. (1992) utilized a second order formulation. More recently, Bracaglia et al. (1995) used the doubling of the transmission and scattering matrices for the calculation of the microwave scattering and emission. The advantage of using the matrix doubling algorithm is that it is able to account for multiple scattering effects. This model has been applied for this thesis and is hereafter referred to as the Tor Vergata model.

1.2. Thesis contribution

In this research, discrete medium vegetation scattering Tor Vergata model has been applied with three different set of configurations. First is the standard configuration by The Tor Vergata model Bracaglia et al. (1995). Second, a beta version developed by us in order to include the latest soil and vegetation dielectric model by Mironov et al. (2002) and Matzler (1994) respectively within the Tor Vergata model. Finally, new version of Tor Vergata model that includes Fraction Vegetation Cover effect is employed through an empirical equation relating it to Leaf Area Index. Data set used to evaluate Tor Vergata model and its new modifications is collected by The NASA-George Washington University truck mounted scatterometer. The collected microwave measurements were during a field campaign covering the 2002 corn growing season at OPE³ test site at dual polarized L-band (1.6 GHz) (A. T. Joseph, van der Velde, O'Neill, Lang, & Gish, 2008).

1.3. Problem definition

The backscatter measurements are affected by vegetation. There are different types of scattering caused by vegetation. Some of them contribute to the soil moisture sensitivity of measurements; others reduce the backscatter sensitivity to soil moisture. These different contributions change during growing season. A better understanding of the changing scattering mechanism throughout the growth cycle can contribute to improve vegetation corrections and, as such, more accurate soil moisture retrievals.

1.4. Research objective and questions

This research objective is employing the discrete medium scattering Tor Vergata model by Bracaglia et al. (1995) for simulating L-band active microwave measurements collected throughout the corn growth cycle to obtain a better understanding for the vegetation effects during the corn growth cycle.

From this objective the following research questions can be formulated:

- Can discrete medium vegetation scattering model be used to model active microwave observations?
- What is the impact of the employed soil and vegetation dielectric model on the simulated backscatter?
- How does the vegetation geometry (e.g. orientation of stems and leaves) affect the simulated backscatter?
- How does the Fraction Vegetation Cover (e.g. orientation of stems and leaves) affect the simulated backscatter?
- Which scattering component dominates the backscattering throughout various parts of the growth cycle?

1.5. Thesis outline

Chapter (1) is the introduction for the research, including the problem definition and the research questions. Chapter (2) gives an overview of the experimental data sets and study area. Chapter (3) summarizes the state of the art of different dielectric models and how it works inside the discrete medium scattering models. Chapter (4) summarizes the Tor Vergata model and describes the approaches that will be adopted to represent the electromagnetic properties of leaves and stems. Chapter (5) provides input data for application of Tor Vergata model. Chapter (6) will discuss the research method for carrying out the backscatter simulation. Chapter (7) will discuss responsibility of different backscattering components in the total backscattering. Finally, Chapter (8) will provide research conclusions.

2. MATERIAL

2.1. Study area description

The study area is the Optimizing Production Inputs for Economic and Environmental Enhancement (OPE³) test site managed by the USDA-ARS (United States Department of Agriculture-Agricultural Research Service). Figure (2-1) shows the study area that includes four adjacent watersheds with similar surface and sub-surface soil and water flow characteristics with total area = 25 ha. Each of the four watersheds was formed from sandy fluvial deposits and has a varying slope ranging from 1% to 4%.

The research site is about 40 m above sea level. A clay lens is under the entire site at depths varying from 0.9 m to 3.5 m below the soil surface. The soil texture in this portion of the field is classified as sandy loam with on average 23.5% silt, 60.3% sand, 16.1% clay and a measured bulk density of 1.25 g cm⁻³. The climate of this region can be characterized as humid with mild winters and hot (and humid) summers. Annual amount of rainfall is about 990 mm evenly distributed throughout the year (A. T. Joseph, Van der Velde, O'Neill, Lang, & Gish, 2010). Other details about this test site can be found at <http://hydrolab.arsusda.gov/ope3/>



Figure (2-1) Location of OPE³ study area

2.2. Data sets

Radar measurements

During the 2002 OPE³ campaign the NASA/George Washington University (GWU) truck mounted scatterometer shown in Figure (2-2) (now called: ComRad) collected active microwave signatures. The scatterometer measured quad-polarized (HH, VV, HV, VH) L-band (1.6 GHz) backscattering coefficients (σ°) at three incidence angles (15, 35, 55) degrees from a boom height of (12.2 m). The radar data acquisition took place once a week resulting in a total of 21 days from emergence of the corn plants (May 15th) till the harvest (October 2nd). Figure (2-3) shows a schematization of this experimental setup where the footprints of a single sample are estimated to be 2.75, 3.83 and 7.98 m for incidence angles of 15, 35 and 55 degrees respectively.



Figure (2-2) The truck mounted radar/radiometer system called ComRad

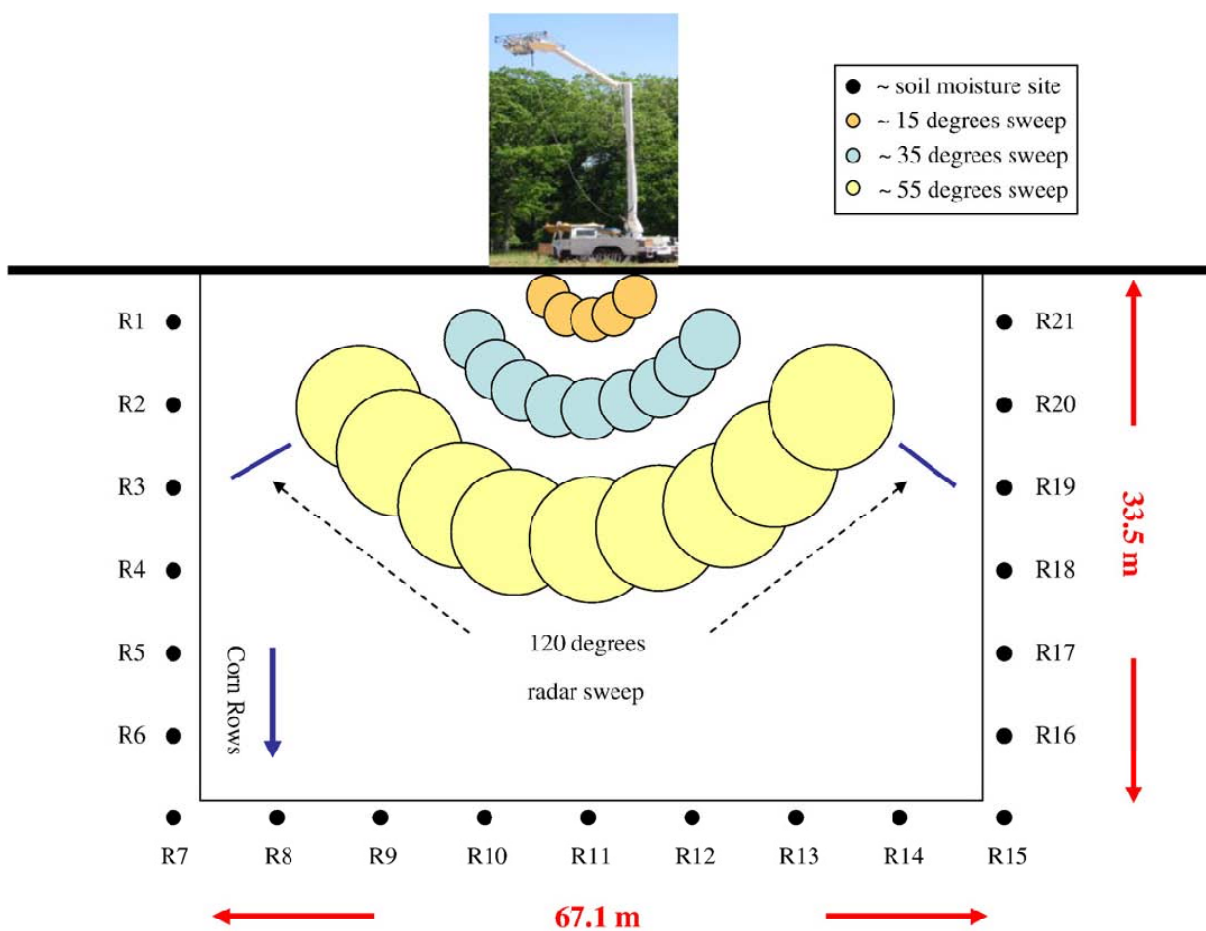


Figure (2-3) Schematization of the experimental setup during 2002 OPE³ field campaign

Vegetation measurements

Throughout the campaign, vegetation biomass and morphology were collected about once a week. The vegetation biomass was quantified once on each radar acquisition day via a destructive sampling technique applied to a (1 m²) area (about 12 corn plants). Figure (2-4) shows the measured values of moisture content of different plant elements for fresh and dry biomass. Leaves have moisture content with minimum (0.17, 0.26 kg m⁻³) and maximum (1.24, 0.35 kg m⁻³) for fresh and dry biomass respectively. However, for stems and cobs moisture content was with minimum (0.18, 0.01 kg m⁻³) and with maximum (5.55, 2.4 kg m⁻³) for fresh and dry biomass respectively. The moisture content for fresh biomass increases from the initial stage till peak biomass and starts to decrease again near senescence. However, for dry biomass the moisture content has a late peak after peak biomass as shown in Figure (2-4) since the corn plant continue growing even water is not there.

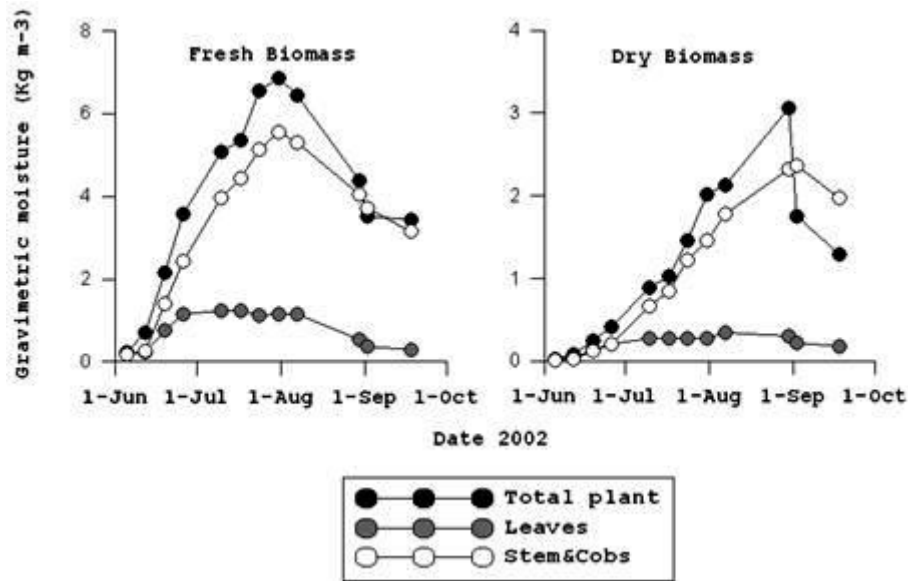


Figure (2-4) Moisture content for corn leaves and stems

The vegetation morphology measurements collected during the OPE³ campaign includes the dimensions of the leaves and stems of a single corn plant. In addition, the orientation of the leaves has also been determined. Figure (2-5) shows geometrical measurements taken for Corn plant elements (stem height, crop height, leaf length, leaf angle). L_{stalk} represents the corn plant height, L_{tip} the represents leaf length, θ_{r} represents leaf inclination angle.

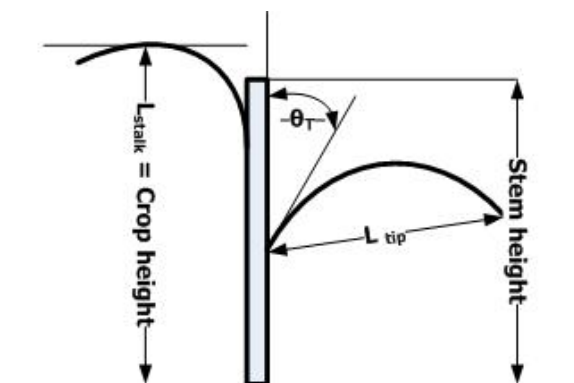


Figure (2-5) Corn geometrical parameters

Figure (2-6) shows measurements of the stem height and the effective radius of the stem. The effective radius of stem is calculated through averaging the minor and major radii of top and bottom of the stem. Stem height increases from the initial stage till near peak biomass rapidly then it increases with lower rate. Near senescence, stem height decreases which may be caused by an increase in stem inclination induced by the loss in stem producing a lower stem height. The effective radius shows a depression in its curve in August since it was a dry period followed by an intensive rain (A. T. Joseph, et al., 2008) so the stem suffers from shrinkage in its radii causing that drop in the effective radius curve and rising it up again.

Figure (2-7) shows measurements of number of leaves, leaves length and width. Number of leaves of corn was counted once a week with minimum of (6 leaves) at initial growth stage and maximum of (12 leaves) from peak biomass up to senescence. Leaves length and width was averaged for all leaves once a week for single plant. They show the same temporal variation, increasing from initial growth up to peak biomass then leaves shows shrinkage in length and width till senescence.

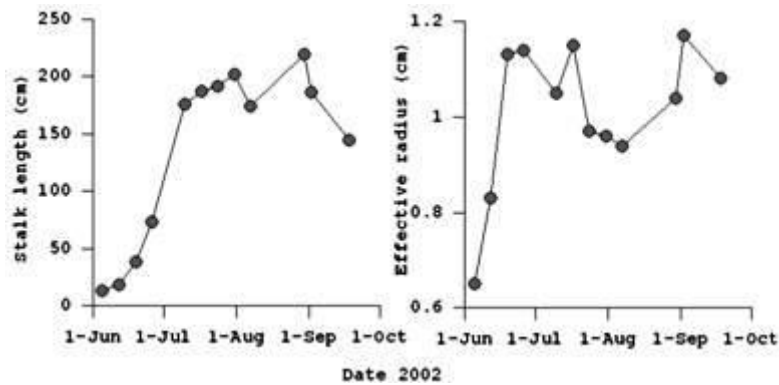


Figure (2-6) Stalk geometry values through the OPE³ campaign

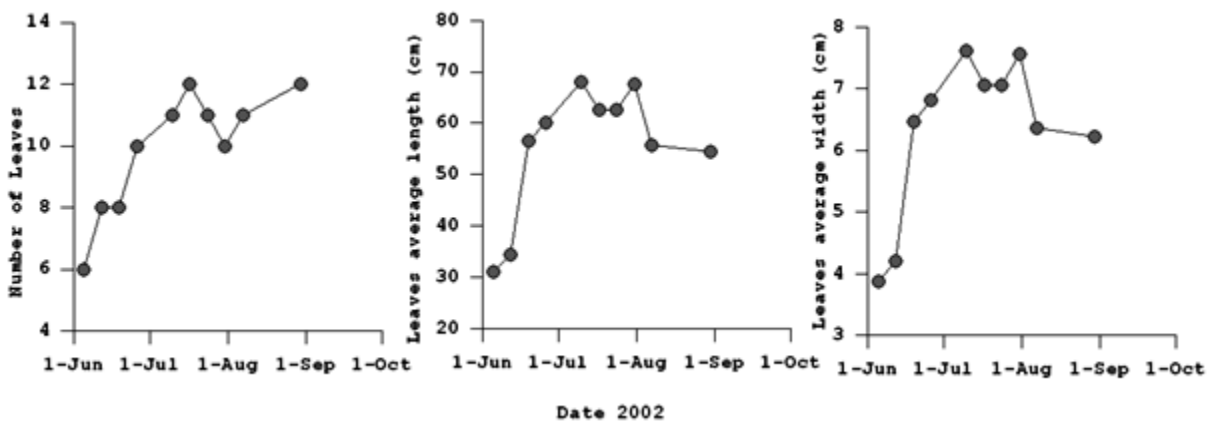


Figure (2-7) leaf geometrical parameters

Soil measurements

Detailed characterization of the land surface conditions took place (e.g. surface roughness, temperature measurements, and soil moisture measurements). Profiles of surface roughness were characterized using 2m long gridded board placed in the soil surface as shown in Figure (2-8).

Soil moisture was measured for the top 6 cm using gravimetric sampling technique and a portable impedance probe (Delta-T theta probe) at 21 sites shown in Figure (2-3). The theta probe observations are calibrated to provide a soil moisture measurement representative for each radar observation. The generalized calibration constants provided by the manufacturer yield an estimated accuracy of ($0.05 \text{ m}^3 \text{ m}^{-3}$). The pair of the gravimetric moisture and the mean of the two simultaneously collected impedance probe readings have been used to fit for each of the twenty-one sites. This led to a Root Mean Squared Difference (RMSD) of ($0.024 \text{ m}^3 \text{ m}^{-3}$) between the gravimetric moisture and the impedance probe moisture (A. T. Joseph, et al., 2010). Figure (2-9) shows the measured soil moisture values. It varies during the campaign period with minimum (1.8 %) and maximum (25.8 %).



Figure (2-8) The 2-m grid board placed in soil surface for characterization of surface roughness

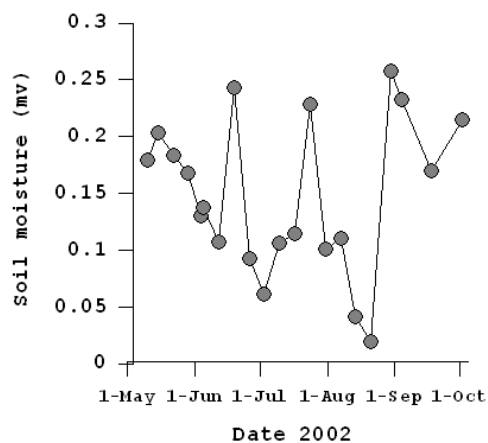


Figure (2-9) soil moisture measured in field

3. BACKGROUND

3.1. Introduction

The active microwave response is related to the vegetation and soil surface properties. Information on the geometric and dielectric properties of the soil surface and the canopy is required to compute individual soil surface and vegetation scattering contributions. The dielectric properties are strongly affected by the water content and the composition of dry material, while the geometry is described by the orientation, size and distribution of vegetation elements and geometry of soil surface.

Interaction between active microwaves and the vegetation layer consists of various scattering terms, see Figure (3-1). In the active microwave observations higher order scattering terms (volume scattering) can be responsible for significant amounts of scattering. In general, microwave backscattering from vegetation covered surfaces considered to be composed of: 1) direct component from the soil surface attenuated by the canopy, 2) direct component from the canopy, and 3) a component direct reflected via the vegetation-soil surface to the sensor as shown in Figure (3-1) and expressed in equation (1).

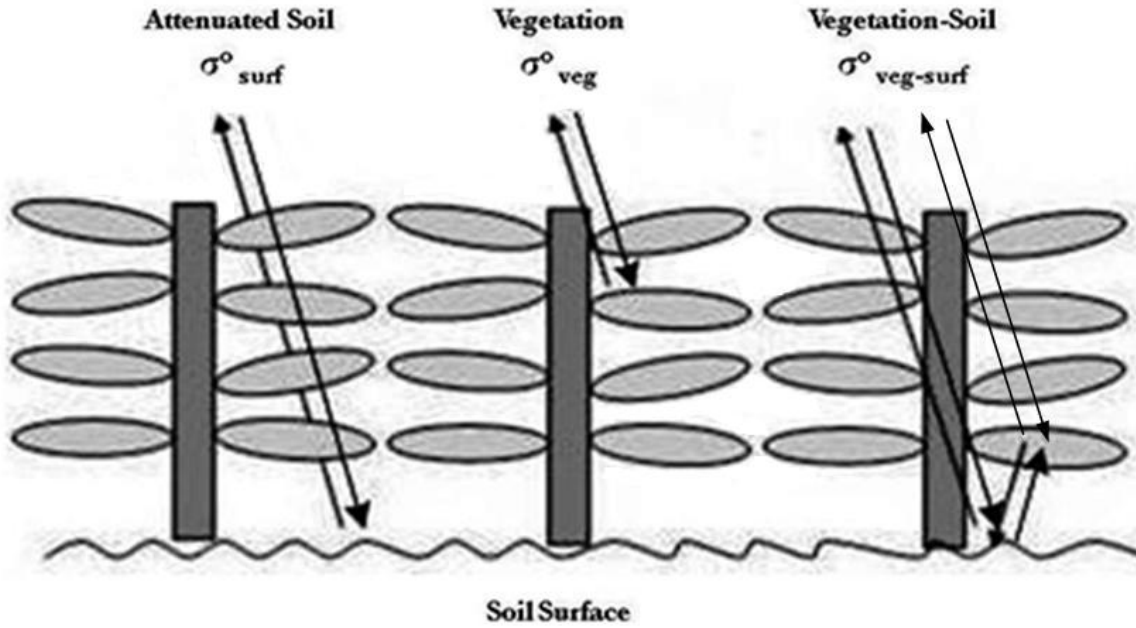


Figure (3-1) Backscattering process over vegetated covered surface affecting active microwave observations

$$\sigma^0 = \sigma_{surf}^0 + \sigma_{veg}^0 + \sigma_{veg-surf}^0 \quad (1)$$

σ_{surf}^0 due to backscatter by the underlying soil surface which is attenuated by vegetation. However, The attenuation in general, is a function of the vegetation parameters (plant height, density, water content, and shape) and the radar parameters (F. T. Ulaby, Bradley, & Dobson, 1979). σ_{veg}^0 due to backscatter by the vegetation and $\sigma_{veg-surf}^0$ is the vegetation surface interaction component.

Surface scattering:

In general, the geometric properties of a rough surface are characterized in terms of three surface roughness parameters: root mean square of height variations, the correlation length and the distribution function. The dielectric properties of a soil surfaces depend on the moisture content and the texture. However, rough surfaces shows higher backscatter response than smooth surface.

Vegetation scattering:

Vegetation scattering depends on the geometry and the density of the canopy layer. The interaction between different components of the vegetation layer and microwave radiation is difficult to describe mathematically and requires an extensive parameterization. The vegetation cover attenuates the surface scattering response and contributes to the total amount of scattering by the radiation scattered back by the vegetation. The attenuation by vegetation and scattering contribution of vegetation decreases as the frequency is lower and it is expected that the retrieval of soil moisture will be more accurate at low frequencies.

3.2. Scatterers representation

Within physically based vegetation models, computation of the scattering contributions described in Eq. 1 and illustrated in Figure (3-1), is based on the dielectric properties, size and orientation of a specific type of scatterer represented by a predefined shape. For example, Stalks can be simulated as cylinders using the infinite length theory (Karam & Fung, 1988; Seker & Schneider, 1988). Leaves are modelled as circular discs using the physical optics theory at high frequency domain (LeVine, Meneghini, Lang, & Seker, 1983) and the Rayleigh-Gans theory at low frequencies (Eom & Fung, 1984; Schiffer & Thielheim, 1979). Suitable electromagnetic theories are used to compute their absorption and scattering cross sections, as well as interactions with soil and other scatterers.

After the electromagnetic properties of the individual scatterers with the canopy are quantified, their combined effect should be integrated over the entire vegetation layer. Then, the computation of the backscatter coefficient with a discrete medium approach can be either based on the wave theory e.g. (Chauhan, et al., 1994) or the radiative transfer theory e.g. (Bracaglia, et al., 1995; Karam, et al., 1992). In the current research the radiative transfer theory is adopted.

3.3. Dielectric models

Soil dielectric models are considered the essential part of many algorithms for retrieving soil moisture from remote sensing data (F.T. Ulaby, Moore, & Fung, 1981). Moreover, the dielectric properties of vegetation material play a central role in coupling between the electromagnetic properties of a vegetation canopy and its physical properties. The dielectric constant of a leaf is governed by its water content and salinity. So, the dielectric constants, shapes, and orientations of the vegetation elements together control the scattering and emission by the canopy (El-Rayes & Ulaby, 1987) .

Soil

Hallikainen et al. (1985) conducted dielectric constant measurements over the (1-18) GHz region for five different soil types. The microwave dielectric behaviour of soil-water mixtures evaluated as a function of water content, temperature, and soil texture. Afterwards, polynomial expressions were developed expressing soil dielectric constant dependent upon the volumetric moisture content and the percentage of sand and clay contained in the soil.

The semi-empirical mixing dielectric model (SMDM) introduced by Dobson, et al. (1985) has been considered “Universally recognized standard” for obtaining the soil permittivity . Dobson relates soil moisture and microwave dielectric properties based upon the index of refraction. It requires only soil physical parameters such as volumetric moisture and soil textural composition as inputs to predict soil's dielectric behaviour for use in microwave scattering calculations. That was fulfilled using Birchak, et al. (1974) approach which apportions the soil solution into bound and bulk water volume fraction. Detailed equations about the semi-empirical model used in the current research can be found in (F.T. Ulaby, et al., 1981).

In 2002 (Mironov, et al.) implemented the complex dielectric constant (CDC) for moist soil. It is based on frequency through the spectroscopic parameters related to the bound and free water in soil. These parameters can be derived from the empirical soil complex refractive index (CRI) dependence on moisture.

The spectroscopic parameters of the Generalized Refractive Mixing Dielectric Model (GRMDM) by Mironov were correlated with the clay percentages of the respective soils in (SMDM) by Dobson. As a result, a new mineralogy based dielectric model was developed. The explicit distinction between the electromagnetic properties of bound and free water added complexity to Mironov's model. However, (GRMDM) model shows a smaller error of dielectric predictions with clay percentage being the only input parameter, as compared with the error in the case of the (SMDM) by Dobson. Accordingly, it gives more accurate estimates of the soil permittivity (Mironov, Kosolapova, & Fomin, 2009).

This enhancement by Mironov, et al. (2002; 2009) showed, however, that the permittivity's obtained with Dobson's model tend to overestimate the measurements for the soils, whose dielectric data were not used for its development. The Generalized Refractive Mixing Dielectric Model (GRMDM) by Mironov, et al. (2002) ensured dielectric predictions for all the soils analyzed with as small error as the (SMDM) did in the case of the soils that it was based on.

Vegetation

Ulaby & El-Rayes (1987) evaluates the microwave dielectric behaviour of vegetation material as a function of water content, microwave frequency, and temperature. They developed a dielectric mixing model for vegetation assuming linear, empirical relationships between vegetation permittivity and volume fractions of free water, bound water, and a residual component. Corn leaves and stems have been considered for that model. For distribution of water in vegetation, they assumed that most of the water is in bound form when water content is low and in free form when the water content is high. As, there were no verifiable models exist that define how the water should be apportioned between the two forms.

Moreover, Matzler (1994) found that for leaves with high water content and for frequencies above 20 GHz Ulaby & El-Rayes model may not be applicable. So, a semi-empirical formula for the complex dielectric permittivity of fresh leaves from different plants was derived by Matzler (1994). This formula is simpler than an earlier expression derived by Ulaby & El-Rayes (1987) since it depends only on two explicit variables. Density was an additional parameter, effect by bound water was hypothesized and density was not significant variable for leaves (Matzler, 1994).

4. TOR VERGATA MODEL

In this research the discrete medium scattering model developed at the Tor Vergata University in Rome (Italy) (Bracaglia, et al., 1995) is used to simulated L-band backscatter coefficients. This model employ a radiative transfer approach and utilizes the matrix doubling algorithms to integrate the scattering and absorption coefficients over the canopy. Leaves are modelled as circular discs using the Rayleigh-Gans approximation at frequencies lower than 5 GHz (Eom & Fung, 1984; Schiffer & Thielheim, 1979) and the infinite length approximation is utilized for the cylinders (Karam & Fung, 1988; Seker & Schneider, 1988).

4.1. Geometric representation

Soil

Within the Tor Vergata model, the soil is represented as a homogeneous dielectric half space with rough interface as shown in Figure (4-1). However, the bistatic scattering coefficient of soil is computed by means of the integral equation model (IEM) developed by Fung (1994; 1992) with an exponential autocorrelation function.

Vegetation

The Tor Vergata model represents vegetation canopy as a unique layer filled with discrete scatterers of discs for describing leaves and cylinders for describing stems as shown in Figure (4-1). It was verified that the inclusion of ears affects the simulations of corn backscattering by less than (0.3 dB) (Della Vecchia et al., 2006). Here, long leaves have been subdivided into several discs, with the diameter equal to the leaf width which corresponds to the assumption proposed by Della Vecchia, et al., (2006). Then contributions of the various scatterers are combined via the “so-called” Matrix Doubling algorithm that includes multiple scattering effects (Bracaglia, et al., 1995).

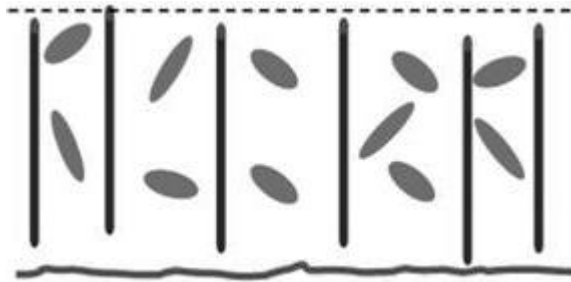


Figure (4-1) Corn Canopy model (Della Vecchia, et al., 2006)

4.2. Dielectric representation

Soil

The Integral Equation Model (IEM), surface scattering model by Fung, et al. (1992) is utilized within the Tor Vergata model to quantify the amount of surface scattering. As input the IEM requires soil variables defining the surface geometry and the soil permittivity.

The surface geometry is based on the representation of the surface height variations. This characterization consists of three parameters, the root mean square height (s), autocorrelation length (l) and autocorrelation function (ACF). The parameters, s and l , are input to the model, while the ACF is typically fixed as being either a Gaussian or an Exponential function. The Tor Vergata model simulations presented in this thesis

are performed using only the Exponential ACF's because this shape has been found to be most appropriate for smooth agricultural surfaces (Davidson et al., 2000).

However, Soil permittivity is calculated within the Tor Vergata model using the semi-empirical dielectric mixing model developed by Dobson, et al. (1985) and also the generalized refractive dielectric mixing model by Mironov et al. (2009) has been included in the Tor Vergata model. Both mixing models are considered for the simulations presented in this thesis.

Vegetation

The Tor Vergata model calculates the permittivity of scatterer within the vegetation layer using either the semi-empirical model given by Ulaby & El-Rayes (1987) or the model by Matzler (1994). Both need moisture content and dry matter density to compute the permittivity as a function of the fresh and dry biomass.

4.3. Integrating the effect of different scatterers

Within the Tor Vergata models the matrix doubling algorithm by Eom & Fung (1984) is used to integrate the scattering and absorption coefficient. The advantage of this approach is the incorporation of the multiple scattering effects. The Tor Vergata model applies the matrix doubling algorithms twice: 1) among individual scatterers in the canopy, and 2) between the canopy and soil surface (Della Vecchia, et al., 2006).

The idea in matrix doubling algorithm, is dividing the vegetation layer into several sub-layers and to characterize the scattering in the upper and lower half spaces associated to each sub-layers. Accordingly, the electromagnetic behaviour of the dielectric bodies, which compose the sub-layer, must be first characterized. Figure (4-2) shows the representation of a scatterer sub-layer (Bracaglia, et al., 1995) where:

- θ_j & θ_{si} : discretized off-normal angles of incidence and scattering directions.
- φ_j & φ_s : azimuth angles of incidence and scattering directions.
- I_{jq} : q-polarized incident specific intensity.
- I_{sip} : p-polarized upward scattered specific intensity.
- I_{tip} : p-polarized downward scattered specific intensity.

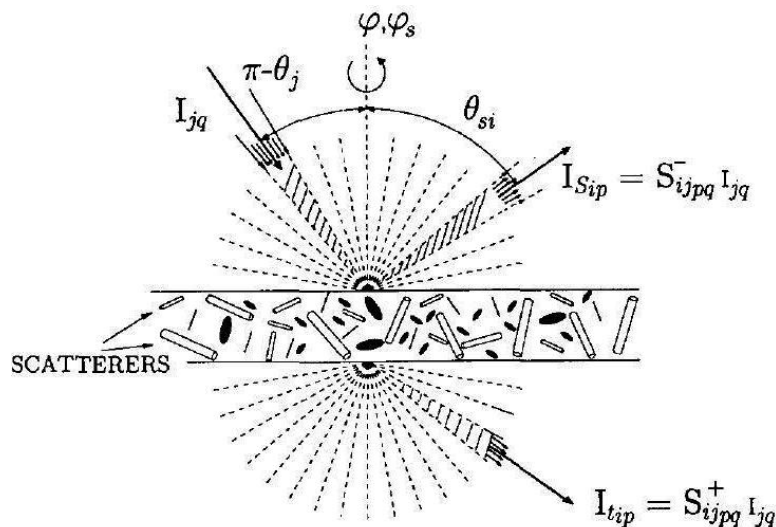


Figure (4-2) Scattering mechanism in the matrix doubling algorithm (Bracaglia, et al., 1995)

The canopy layer is divided into N thin sub-layers with thickness Δz as shown in Figure (4-3). The number N is selected as the minimum value beyond which the finally computed backscatter coefficient does not vary by more than a given limit (e.g., 0.5 dB) (Bracaglia, et al., 1995). Then, the scattering and absorption matrices of a single layer for downward travelling radiation can be defined as,

$$S = M^{-1}K_e P(\mu_s, -\mu_i, \varphi_s - \varphi_i)\Delta z \quad (2)$$

$$T = M^{-1}K_e P(\mu_t, -\mu_i, \varphi_t - \varphi_i)\Delta z \quad (3)$$

where, S is the scattering matrix, T is the transmission matrix, M is the diagonal matrix of directional cosine, K_e is the extinction matrix, P is the phase matrix, μ is cosine of the angle between z -axis and wave, φ is the angle between the wave and x -axis and subscripts i , s , and t indicate the incident, scattered and transmitted energy.

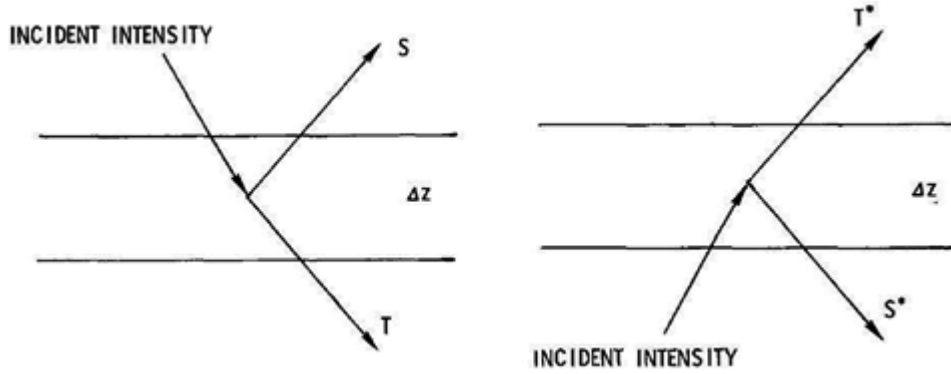


Figure (4-3) Scattering and transmission matrices for downward (left) and upward (right) travelling radiation (Eom & Fung, 1984)

For upward travelling radiation the scattering and transmission matrices can be defined as,

$$S^* = M^{-1}K_e P(\mu_s, -\mu_i, \varphi_s - \varphi_i)\Delta z \quad (4)$$

$$T^* = M^{-1}K_e P(\mu_t, -\mu_i, \varphi_t - \varphi_i)\Delta z \quad (5)$$

Through the combination of the scattering and transmission matrices for downward and upward travelling radiation of two layers with thickness Δz as shown in Figure (4-4), the S , T , S^* and T^* can be computed for a layer of thickness $2\Delta z$ as follows,

$$S = S_1 + T_1^* S_2 (I - S_1^* S_2)^{-1} T_1 \quad (6)$$

$$T = T_2 (I - S_1^* S_2)^{-1} T_1 \quad (7)$$

$$S^* = S_1^* + T_1 S_2^* (I - S_1 S_2^*)^{-1} T_1^* \quad (8)$$

$$T^* = T_2^* (I - S_1 S_2^*)^{-1} T_1^* \quad (9)$$

Where, I represent the identity matrix.

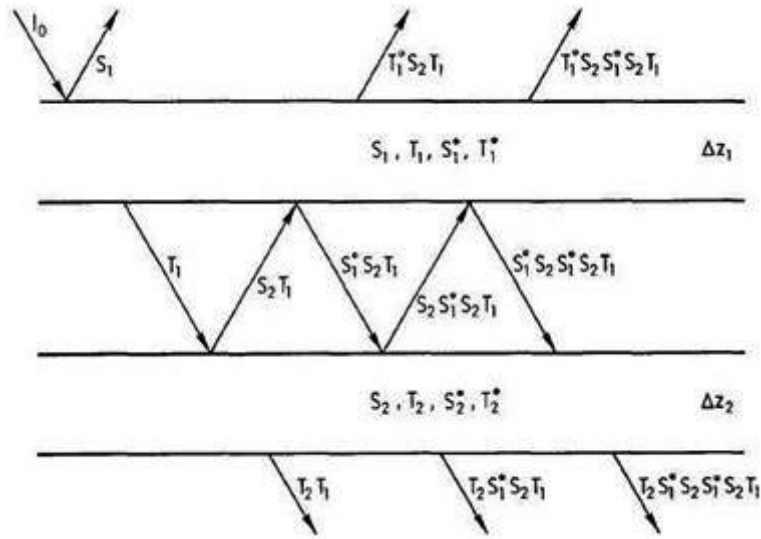


Figure (4-4) Scattering process for unit incident intensity

When layer 1 and layer 2 are identical in property, (i.e., $S_1 = S_2$, $T_1 = T_2$, etc., and $\Delta z_1 = \Delta z_2$), then equations 12,13,14,15 represent the phase matrices for the doubled layer. This process can be repeated to obtain the phase matrices of a medium with any thickness.

The scattering and transmission matrices of the upper layer and of the lower layer are calculated, and doubling the two layers, the whole vegetation layer is built and the average polarized bistatic scattering cross sections in the upper and lower half-spaces is obtained. A scattering matrix for the soil—proportional to the soil bistatic scattering coefficient—is calculated, and the same matrix doubling algorithm is then applied to combine soil and vegetation scattering (Della Vecchia, et al., 2006).

4.4. Backscatter calculation over closed canopies

Once the scattering and transmission matrices have been integrated over the entire vegetation layer, the total scattering matrix (S_T) can be calculated using,

$$S_T = S_{veg} + T_{veg}^* S_{soil} (I - S_{veg}^* S_{soil}) T_{veg} \quad (10)$$

Where, subscripts (veg and soil) indicate that the property is defined for the vegetation layer or the soil surface, respectively. The first term on the right-hand side represents the direct vegetation term, while the second term includes the soil scattering contribution attenuated by the canopy and scattering along the soil-vegetation pathways.

From the k_{th} row and l_{th} column element of the p, q polarized stokes parameter in S_T ; the bistatic scattering coefficient $\sigma_{pq}^0(\theta_{sk}, \theta_s, \varphi_s - \varphi)$ can be obtained as follows,

$$\sigma_{pq}^0(\theta_{sk}, \theta_l, \varphi_s - \varphi) = \frac{4\pi}{\Delta\theta} \cot \theta [S_T(\theta_{sk}, \theta_l, \varphi_s - \varphi)]_{pq} \quad (11)$$

4.5. Backscatter calculation over open canopies

Discrete medium scattering models considered the soil to be fully covered by vegetation ($FVC = 1$). However, it is often not the case. The vegetation is not fully covering the soil surface; the backscatter can be calculated using equation (1) section 3.1 whereby the first term is computed using the IEM model and the other two components are determined by the Tor Vergata model.

Fraction vegetation cover (FVC) to be given as inputs to the Tor Vergata model, have been related to leaf area index (LAI) by empirical relationships (Choudhury, 1987) as follows,

$$FVC = 1 - (\exp (0.5 * LAI)) \quad (12)$$

5. APPLICATION OF TOR VERGATA MODEL

The Tor Vergata model requires, as input, the geometric and dielectric variables of soil and vegetation. We have used the measured ones and, if not available, we have estimated them. Variables influencing backscattering are shown in Table (5-1) they are used as inputs for TorVergata model. Most of the mentioned model inputs have directly been derived by ground measurements.

Table (5-1) Inputs for TorVergata model

Dielectric	Soil	Average daily soil moisture and texture.
	Vegetation	Average daily moisture content stems and leaves, Biomass
Geometry	Soil	IEM roughness (surface height standard deviation, correlation length) and it is assumed to be invariant through the growth cycle of corn (A. T. Joseph, et al., 2010) (Along row average for 5 profiles)
	Vegetation(Plant morphological parameter)	<ul style="list-style-type: none"> • Stem parameters: (Shape, dimensions, orientation) <ul style="list-style-type: none"> • Plant density (12 per square meter) • Stem radius • Stem length • Angles in azimuth • Angles in the vertical • Leaf parameters: (Shape, dimensions, orientation) <ul style="list-style-type: none"> • Calculated LAI • Leaf width (disc radius) • Leaf thickness • Angles in azimuth • Angles in the vertical
Incidence Angles		15,35,55 degrees
Microwave frequency	L-Band	1.6 GHz

Some parameters have been assumed to be constant, since they showed relatively small variations during the campaign period:

- Soil roughness standard deviation : (RMS = 0.872)
- Soil roughness correlation length : (L = 5.132)
- Stalk (Stem) density: $N_s = 12 \text{ per m}^2$
- Disc (leaf) thickness: = 0.02 cm

Leaves of the corn canopy is parameterized by the leaf area index (LAI), leaf thickness and disc radius. LAI was not directly measured but derived from leaf dimensions measurements. Disc radius is equal to half leaf width and a fixed leaf thickness of 0.2 mm is used. Then, the number of discs within the medium is obtained by dividing the LAI by the disc's surface area.

The stem radius and length define its dimensions and the number of stems is used to quantify the density of the scattering medium. The angles describing the orientation of leaves and stems reasonable assumptions, based on measurements in previous studies (Chauhan, et al., 1994) and field measurements for crop (A. T. Joseph, et al., 2010) have been considered. The minimum and maximum position can be

defined within the Tor Vergata model for leaves and stems. The scattering amplitude functions are averaged over these angles with an interval of 1.0 degree for stems and 5.0 degrees for leaves.

Tor Vergata model has been applied with three different set of configurations:

First is the standard configuration by P.Ferrazzoli, L. Guerriero and M. Bracaglia (1995):

- Fixed maximum stem angle = 5 degrees
- Fixed maximum leaf angle = 85 degrees
- Ulaby & El-Rayes model for vegetation dielectric calculations
- Dobson model for soil dielectric calculations
- Exponential Auto Correlation Function for surface roughness

Second, include the latest soil and vegetation dielectric model by Mironov et al. (2002) and Matzler (1994) respectively within the Tor Vergata model.

- Variable maximum stem angle
- Variable maximum leaf angle
- Including recent vegetation dielectric model by Matzler
- Including recent soil dielectric model by Mironov
- Exponential Auto Correlation Function for surface roughness

Finally, new version of Tor Vergata model considers Fraction Vegetation Cover (FVC) effect is employed through an empirical equation relating it to Leaf Area Index shown in equation (12) section 4.5

- Max stem angle = 10 degrees
- Max leaf angle = 85 degrees
- Matzler vegetation dielectric model
- Mironov soil dielectric model
- Exponential Auto Correlation Function
- Including Fraction Vegetation Cover effect

6. BACKSCATTER SIMULATION

In this Chapter, Tor Vergata model backscattering simulations of the L-band (σ^0) are presented and compared to the measurements collected during the OPE³ campaign. The measured vegetation morphology (described in Chapter 2) has been used as input for these simulations. A shortcoming in this vegetation morphological characterization is, however, the absence of measured soil and vegetation dielectric properties as well as the orientation of scatterers (e.g. Stems and leaves).

Soil and vegetation dielectric mixing models can be used to determine the dielectric constants from the soil moisture and biomass measurements. These mixing models are, however, uncertain. To quantify this uncertainty within the Tor Vergata model, simulations have been performed using the two widely used mixing models for soil and vegetation, which are the ones developed by Dobson (1985) and Mironov et al. (2002) for soils and the ones by Ulaby & El-Rayes (1987) and Matzler (1994) for vegetation.

Similarly, the sensitivity of Tor Vergata model simulations to the orientation of individual scatterers (e.g. leaves, stems) is evaluated. To this aim the effect of the leaf and stem orientation on the simulated σ^0 are analyzed separately.

In addition, a beta version of the Tor Vergata model permits σ^0 simulations for specific vegetation cover fractions. The cover fraction calculated based on LAI (see Section 4.5), used as input for this version of the Tor Vergata and its performance is evaluated.

In the text below the results from these simulations are presented.

6.1. Effects of dielectric models

Figure (6-1) shows both the simulated and measured L-Band ($F = 1.6$ GHz) backscattering against time for incidence angles of 15, 35, 55 degrees at HH & VV polarization. In general, the temporal σ^0 variations simulated by the Tor Vergata model match the measurements reasonable well.

During the initial growth stage of corn in the first three weeks, For HH polarization, the simulated σ^0 is close to the measured backscattering which demonstrates that the measured roughness parameters is representing well the surface conditions. In addition, for VV polarization Tor Vergata model tends to overestimate the σ^0 by 7 to 9 dB for the higher incidence angles (i.e. 35 & 55 degrees) in the first two weeks but in the third week σ^0 values are getting close again to the measured ones with 2 dB differences.

Near to peak biomass the simulated VV σ^0 agree very well with measurements at all three incidence angle. However, in HH polarization simulations Tor Vergata model tends to overestimate the measurements by up to 13 dB. The latter is elaborated on further below. Near senescence both HH and VV polarized simulations show a large discrepancy with the measurements. This can be explained because at this growth stage the LAI was not measured and assumed the same for the last three weeks.

Four soil and vegetation dielectric models are utilized within Tor Vergata. Matzler's model together with Dobson's model gives closer σ^0 values to the measured ones up to 2 dB than Ulaby & El-Rayes' model with Dobson's model. Furthermore, Matzler's model with Mironov's model, Tor Vergata gives closer σ^0 values to the measured ones than Ulaby & El-Rayes' with Mironov. In conclusion, Matzler's vegetation permittivity approach gives lower σ^0 . This affects mostly the simulations in the period where the corn canopy has large moisture content, which is prior to near peak.

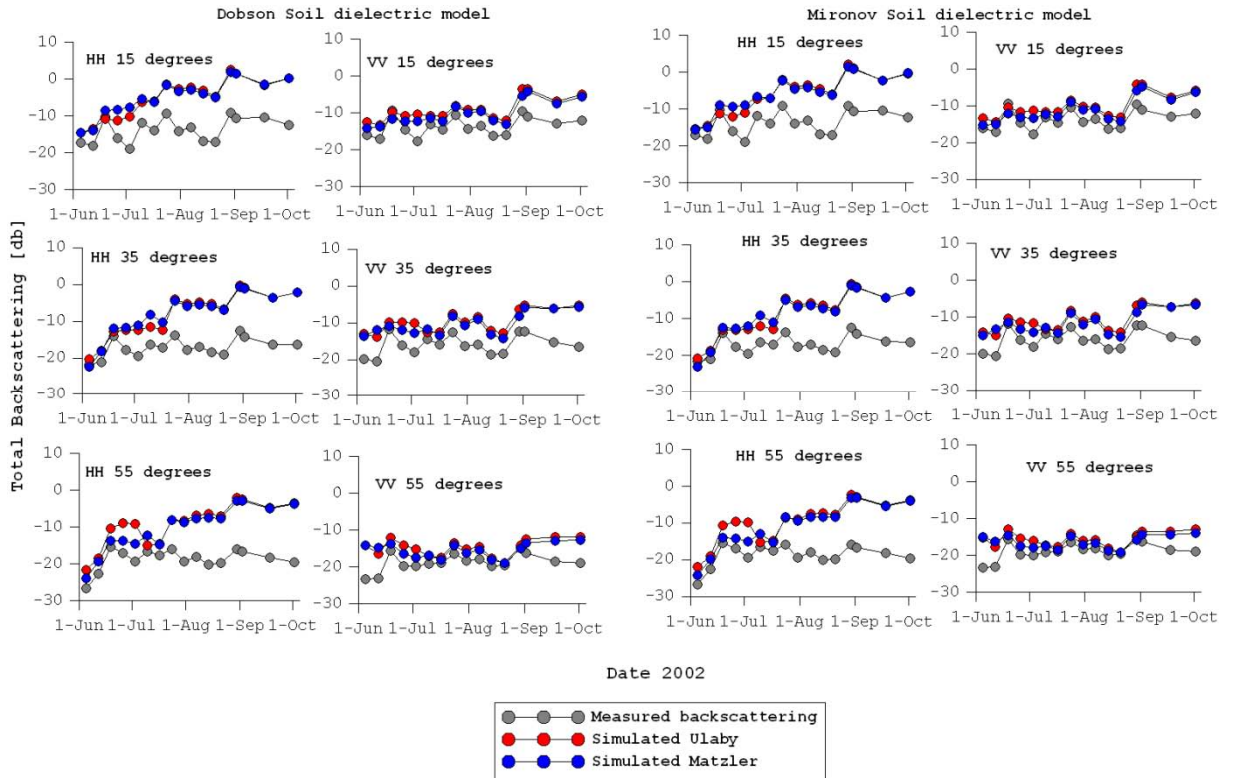


Figure (6-1) Backscatter simulations with measured ones using four dielectric model combinations

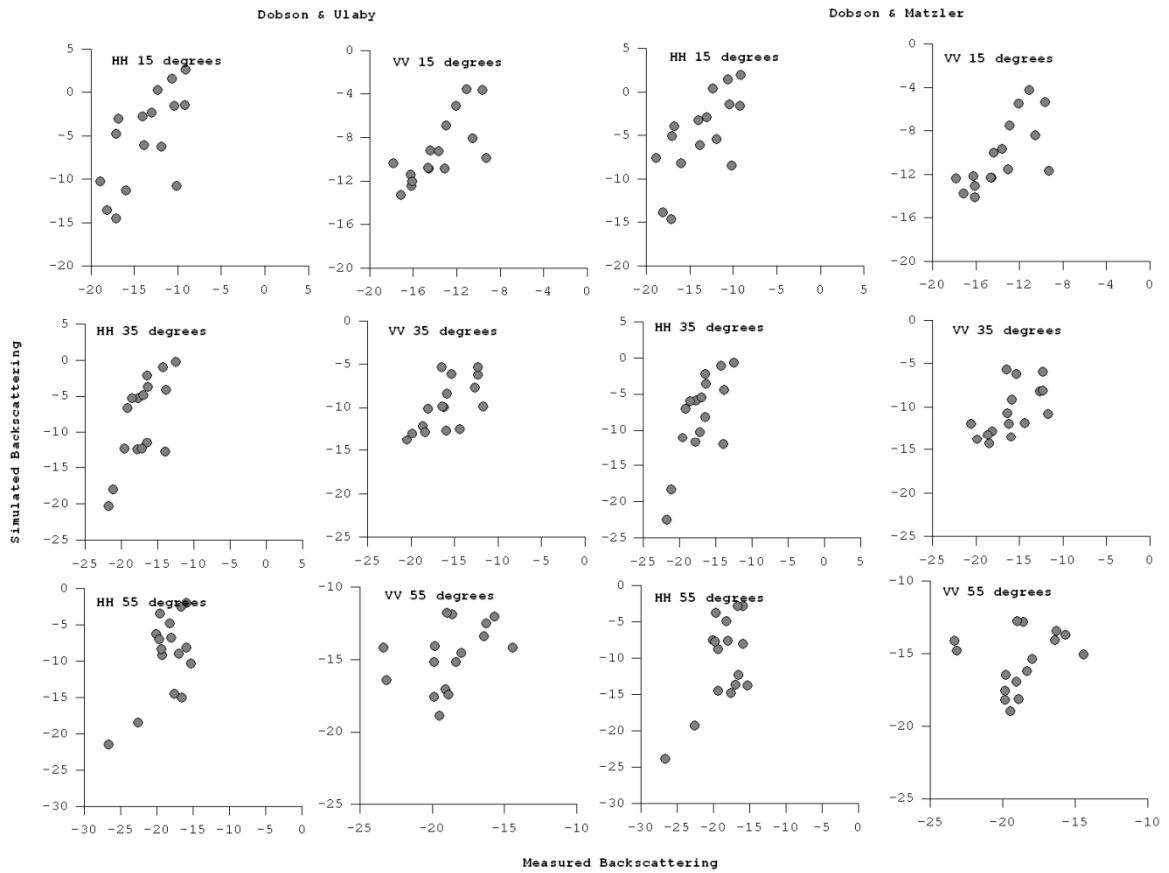


Figure (6-2) measured vs. simulated backscattering for Dobson soil model together with Ulaby & El-Rayes and Matzler vegetation models

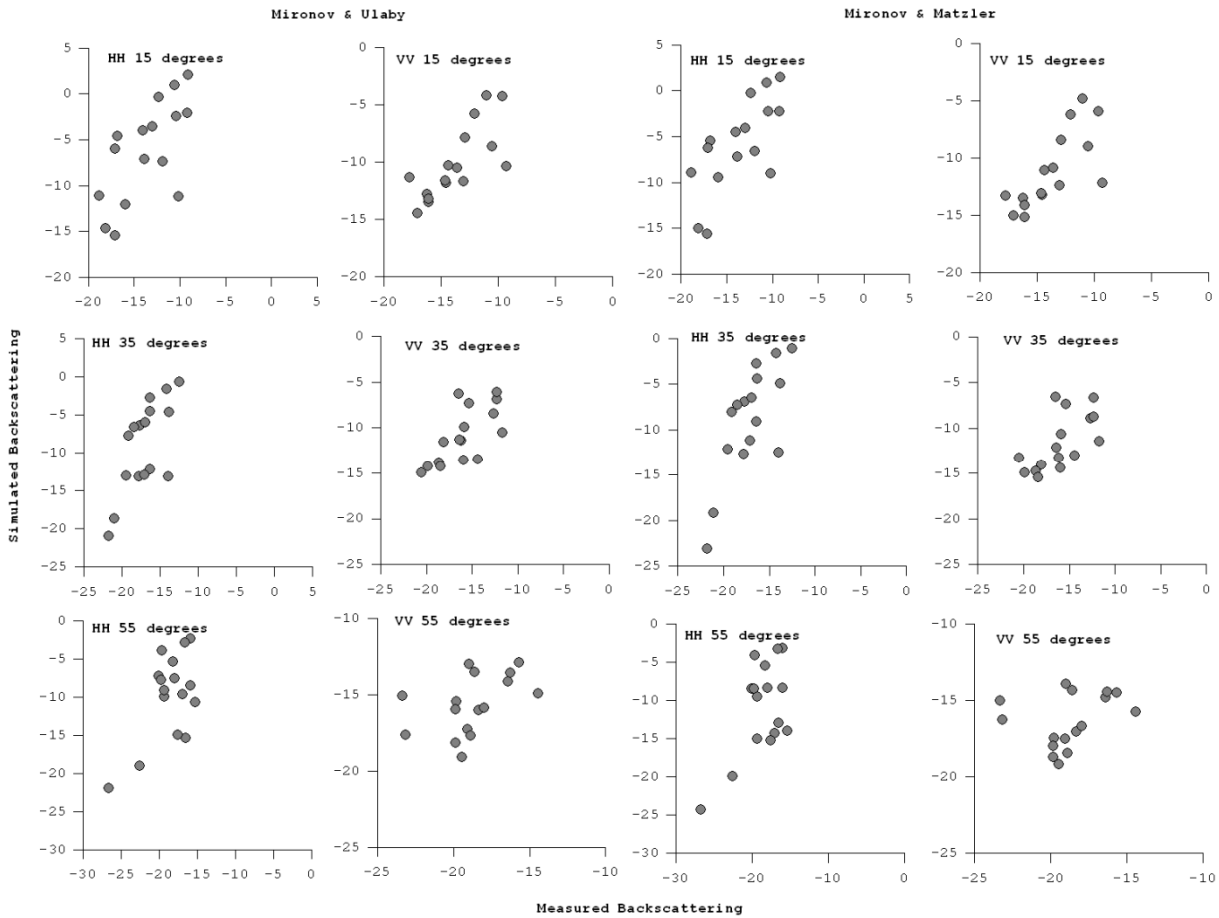


Figure (6-3) measured vs. simulated backscattering for Mironov soil model together with Ulaby & El-Rayes and Matzler vegetation models

For the evaluation of Tor Vergata model performance several statistical measures is used to compare measured and simulated backscattering .For example,

- BIAS: the difference between average simulated and average measured backscattering
- SEE: standard error of simulated backscattering
- RMSD: Root Mean Square Difference
- MAD: Mean Absolute Difference
- R: Correlation Coefficient

Figure (6-2) & Figure (6-3) shows the relation between measured and simulated back scattering for the four soil and vegetation dielectric model combination. Further, Table (6-1) shows several statistics related to the comparison between measured and simulated σ° for four combinations of vegetation and soil dielectric models used within the Tor Vergata model. As expected from Figure (6-1) the error statistics for Matzler's model together with Mironov's model is better than other model combinations. For example, the mean absolute difference (MAD) is 5.64 dB and the Root Mean Squared Difference (RMSD) is 6.45 dB for Matzler with Mironov. Moreover, low SEE of 3.20 dB is noted for that model combination even though it is not the lowest correlated to the measured σ° .

Moreover, Table (6-1) indicates that Matzler model produces better results than Ulaby-El Rayes model within Tor Vergata model. Also, Mironov's soil model shows higher correlated σ° values than that by Dobson's model. This can be explained through conclusions by Mironov, et al. (2009). Their model shows smaller error of dielectric predictions for soils than Dobson's model. That is due to the explicit distinction

between the electromagnetic properties of bound and free water in Mironov's model which is not considered in Dobson model (Mironov, et al., 2009).

In addition, Ulaby & El-Rayes assumed that most of the water in vegetation is in bound form when water content is low and in free form when the water content is high. This assumption produces an error in the predicted dielectric constant for fresh leaves. However, Matzler shows that bound-water effects would have to be considered for dryer leaf material showing lower error of prediction in the dielectric constant (Matzler, 1994).

Further, Table (6-2) also shows that the error statistics for the VV polarized σ^0 are better than that of HH polarization as concluded from Figures (6-1),(6-2) and (6-3). For example, the mean absolute difference is 4.11 dB for VV and 8.47 dB for HH but, a higher R is noted for HH than VV polarization. In conclusion, Matzler's model together with Mironov's model estimates total backscattering from vegetated covered surface better than other model combinations especially at VV polarization for higher incidence angles.

Table (6-1) Average values for statistical measures comparing measured and simulated backscattering for different soil and vegetation dielectric models

	R	BIAS	SEE	RMSD	MAD
Dobson-Ulaby	0.61	-6.91	3.34	7.66	6.93
Dobson-Matzler	0.59	-6.37	3.29	7.21	6.45
Mironov-Ulaby	0.65	-6.08	3.23	6.87	6.13
Mironov-Matzler	0.62	-5.53	3.20	6.45	5.64
Ulaby	0.63	-6.49	3.29	7.27	6.53
Matzler	0.60	-5.95	3.24	6.83	6.05
Mironov	0.64	-5.81	3.22	6.66	5.89
Dobson	0.60	-6.64	3.31	7.43	6.69

Table (6-2) Average values for statistical measures comparing measured and simulated backscattering for HH and VV polarization

	R	BIAS	SEE	RMSD	MAD
VV polarization	0.57	-4.02	2.17	4.66	4.11
HH polarization	0.66	-8.43	4.36	9.43	8.47

6.2. Vegetation geometry effects

According to section 6.1, the lowest differences between simulated and measured σ^0 were noted in case of implementing Matzler together with Mironov permittivity models within Tor Vergata model. Part of the differences is due to uncertainties in the dielectric model. However, the majority of the remaining discrepancies are still high. Another source of uncertainty within these Tor Vergata model simulations is the orientation of scatterers (e.g. stem and leaves).

To investigate this sensitivity of the simulated backscatter, the Tor Vergata model was run using several ranges of leaves and stem inclination angles. These simulations were performed using Matzler's (1994) vegetation permittivity model together with Mironov (2009) soil permittivity model. In the text below these simulations and the results are further described.

Tor Vergata model averages the scattering amplitude functions for both stems and leaves over a range of orientation defined by their minimum and maximum position. Minimum and maximum angles were defined and intervals of (10.0 & 1.0 degrees) were selected for leaves and stems respectively.

Effect of leaf orientation

Variable maximum leaf angles were estimated (85, 60, 45, 30 degrees) with an initial angle of 5 degrees used as an input for Tor Vergata model. These angles agrees with the leaf angle distributions of corn measured in the field (A. T. Joseph, et al., 2010). This simulation was run with fixed stem angles of 15 degrees as maximum angle, 2 degrees as initial angle and an interval of 1.0 degree.

Figure (6-4) shows Tor Vergata model response towards different leaf angle distribution. Tor Vergata model produces almost the same values with the same temporal variation at all leaf angle distributions. This demonstrates that the measured roughness parameters represent well the surface conditions. However, during initial growth stage, the first three weeks, HH polarization at all incidence shows very close σ^0 values to the measured ones with differences up to 2 dB keeping the same temporal variations. Significant differences are still noted in case of VV polarization at higher incidence angles (35 & 55 degrees). Near peak biomass, at VV polarization, simulated σ^0 very close to measured ones with differences within 1 dB. Near senescence large difference up to 8 dB still noted in the simulated σ^0 for both HH and VV polarization.

Table (6-3) shows the statistical measures for comparing simulated backscattering at different maximum leaf angle. All leaf orientations produce almost the same simulated backscattering with similar values of RMSD, BIAS, MAD and R. In conclusion, Tor Vergata model shows no sensitivity to variations in leaf orientations.

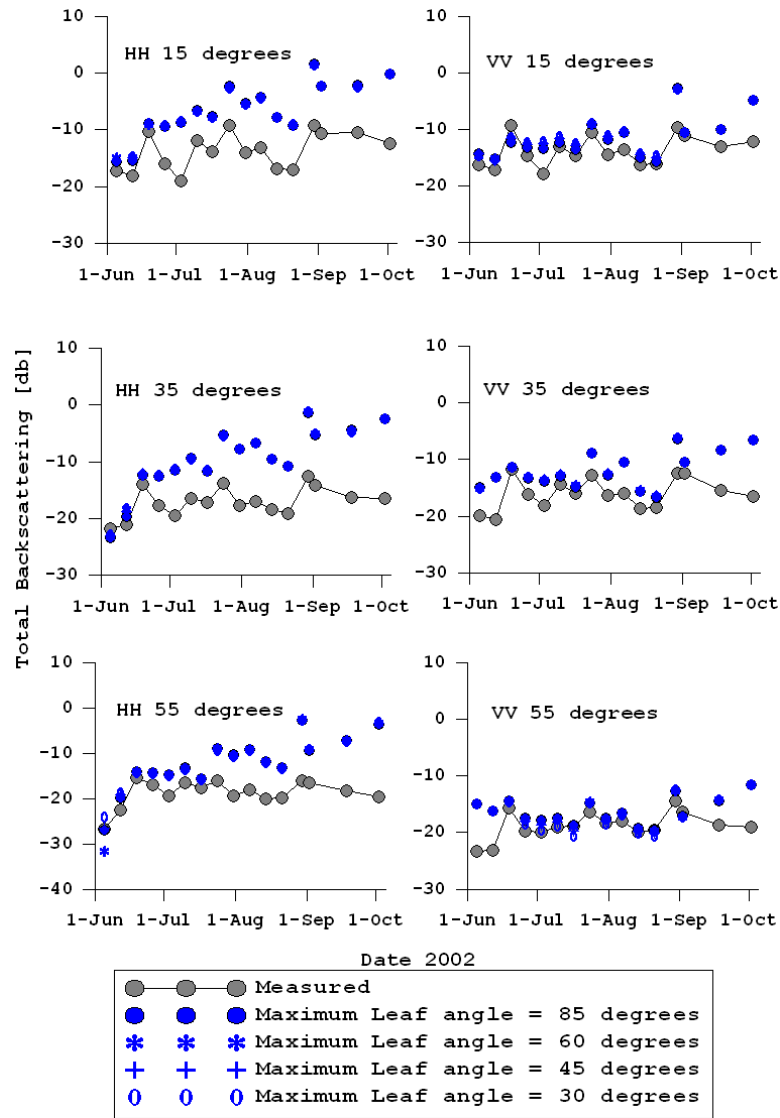


Figure (6-4) Effect of different leaf orientation on Tor Vergata Model

Table (6-3) statistical measures showing sensitivity of Tor Vergata model towards effect of different leaf orientations

Maximum Leaf angle	R	BIAS	SEE	RMSD	MAD
85 degrees	0.64	-4.99	3.18	5.99	5.12
60 degrees	0.65	-5.00	3.20	6.03	5.21
45 degrees	0.64	-5.03	3.16	6.00	5.15
30 degrees	0.63	-5.02	3.18	6.01	5.17

Effect of stem orientation

Tor Vergata model sensitivity to stem orientation needed to be investigated. Accordingly, several ranges of stem orientation is selected and defined by its minimum and maximum position with an interval of 1.0 degree. These angles were estimated based on previous measurements taken by Chauhan (1994) which shows that the inclination angles of corn stalks are uniform within 15 degrees. Leaf angles used for this simulation were with maximum angle of 85 degrees, interval of 10 degrees and with an initial angle of 5 degrees.

The estimated ranges used as input for Tor Vergata model with an initial angle of 2 degrees:

- maximum angle of 5 degrees through whole growth cycle;
- maximum angle of 10 degrees through whole growth cycle;
- maximum angle of 15 degrees through whole growth cycle;
- Several maximum angles, during initial growth stage 2-5 degrees, near peak biomass 2-10 degrees, near senescence stage 2-15 degrees, which is close to the situation in field. At initial growth stage corn stems are vertical and by increasing moisture content of leaves, stem angle varies according to growing stage and moisture content.

Figure (6-5) shows the effect of using several ranges of stem orientations within Tor Vergata model. The simulated HH-polarized σ^0 is more affected by changes in stem orientation than the VV-polarized. At HH polarization, differences in simulated σ^0 values from 5 to 10 degrees and from 10 to 15 degrees maximum stem angle ranges up to 2 dB closer to the measured σ^0 . Besides, at VV polarization, differences between various stem orientations results in less than 1 dB. However, Tor Vergata model at VV polarization at different incidence angles produces closer σ^0 values to measured ones than that produces at HH polarization.

Table (6-4) shows several statistical variables to evaluate the performance of the Tor Vergata model with different stem orientations. The simulated σ^0 with maximum angle of 15 degrees perform best. For example, SEE equal to 2.28 dB, RMSD equal to 4.66 dB and MAD equal to 4.03 dB. The error is still quite high especially near senescence that may be because LAI is estimated to be constant the last three weeks. However, simulations with variant maximum stem angle through the corn growth cycle gives higher $R = 0.67$ with the measured σ^0 . Moreover, using 15 degrees as stem inclination angle within is not reasonable, using the variant stem angle is more reasonable as it represent the case in field.

O'Neill et. al, (1984) concluded that orientation of stalks and their distribution affects the microwave backscattering. This effect varies according to vegetation biomass and soil moisture content. This supports the conclusion that the larger maximum stem angle the lower better simulated σ^0 values by Tor Vergata model.

Further, Table (6-5) shows statistics computed between the measured and simulated HH and VV polarized backscatter. At maximum stem angle of 15 degrees the simulated backscattering shows the lowest differences to the measured ones. Increasing stem angle the simulated HH polarized backscattering is improved as it is more affected by stem orientation However, VV has more chance to reach soil.

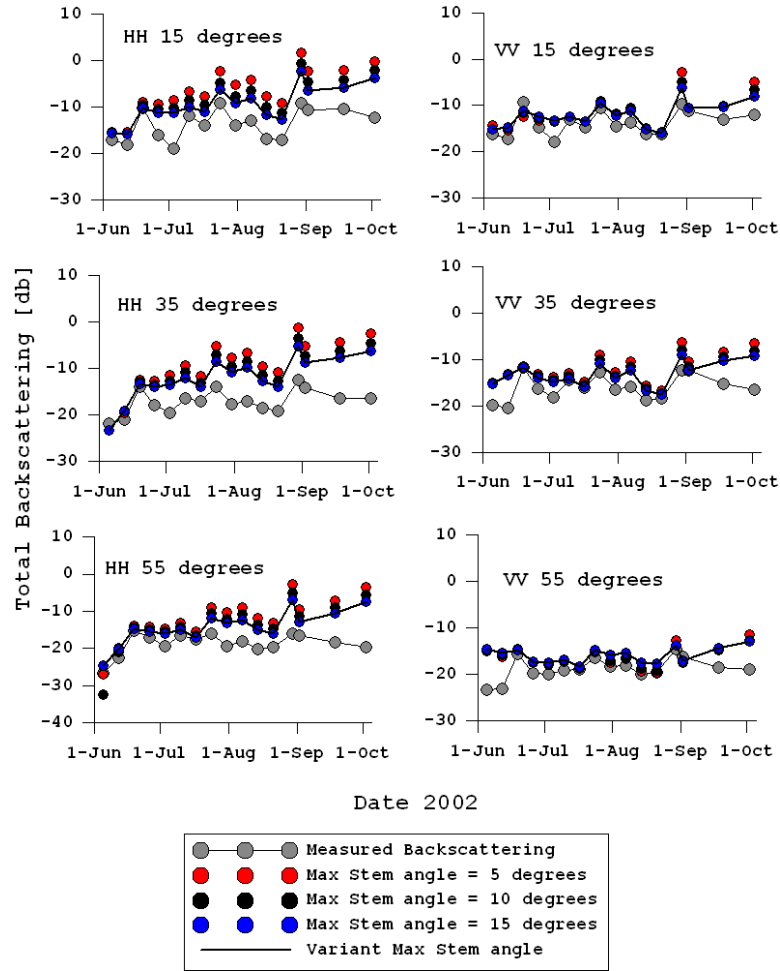


Figure (6-5) Effect of stem orientation on simulated backscattering

Table (6-4) Several Statistical measures to compare measured and simulated σ_0 at different maximum stem angles

	R	BIAS	SEE	RMSD	MAD
Max 5 degrees	0.62	-5.50	3.21	6.43	5.66
Max 10 degrees	0.63	-4.51	2.74	5.36	4.66
Max 15 degrees	0.66	-3.95	2.28	4.66	4.03
Max Variant	0.67	-4.27	2.29	4.94	4.41

Table (6-5) Several Statistical measures to compare measured and simulated σ_0 at HH & VV polarization.

	HH	VV
R	0.72	0.57
BIAS	-6.30	-2.82
SEE	3.51	1.75
RMSD	7.18	3.52
MAD	6.43	2.96

6.3. Effect of fraction vegetation cover

In the previous two sections uncertainties were discussed related to dielectric properties and orientation of scatterers. On the other hand, the Tor Vergata model, like any other discrete medium approach, assumes that the surface is completely covered by vegetation. Recently, the Tor Vergata University developed a new version that includes the vegetation fraction cover (FVC). In this section, this beta version will be evaluated using the Matzler and Mironov (vegetation and soil) dielectric models at variant maximum stem angle through corn growth cycle and leaf maximum angle of 85 degrees. For this simulation the FVC is computed based on the LAI using equation (11) in section 5.

Figure (6-6) shows the effect of FVC on simulated backscattering within the Tor Vergata model. The simulated backscattering in case of including FVC effect produces σ^0 of 1 dB closer to measured ones. However, VV polarization at all incidence angles the simulated backscatter gets closer to measured backscattering with differences up to 2 dB. Moreover, the simulated backscattering at HH polarization shows improvement with closer values to measured ones but still have differences up to HH=5 dB. Discrepancies still there between simulated and measured σ^0 at HH and VV polarization at senescence stage in last three weeks.

Further, Table (6-6) shows some statistical measures between measured and simulated backscattering in case of including FVC and the normal case without FVC. The new version of Tor Vergata model produce simulated backscattering with higher R to measured ones with lower RMSD. For example, RMSD equal to 4.41 dB and MAD equal to 3.80 dB due to including FVC. In conclusion, including FVC effect gives better estimates for the simulated backscattering.

Table (6-6) statistical measures showing the differences between including FVC and the previous version of Tor Vergata model

	No FVC	FVC
R	0.67	0.70
BIAS	-4.27	-3.70
SEE	2.29	2.17
RMSD	4.94	4.41
MAD	4.41	3.80

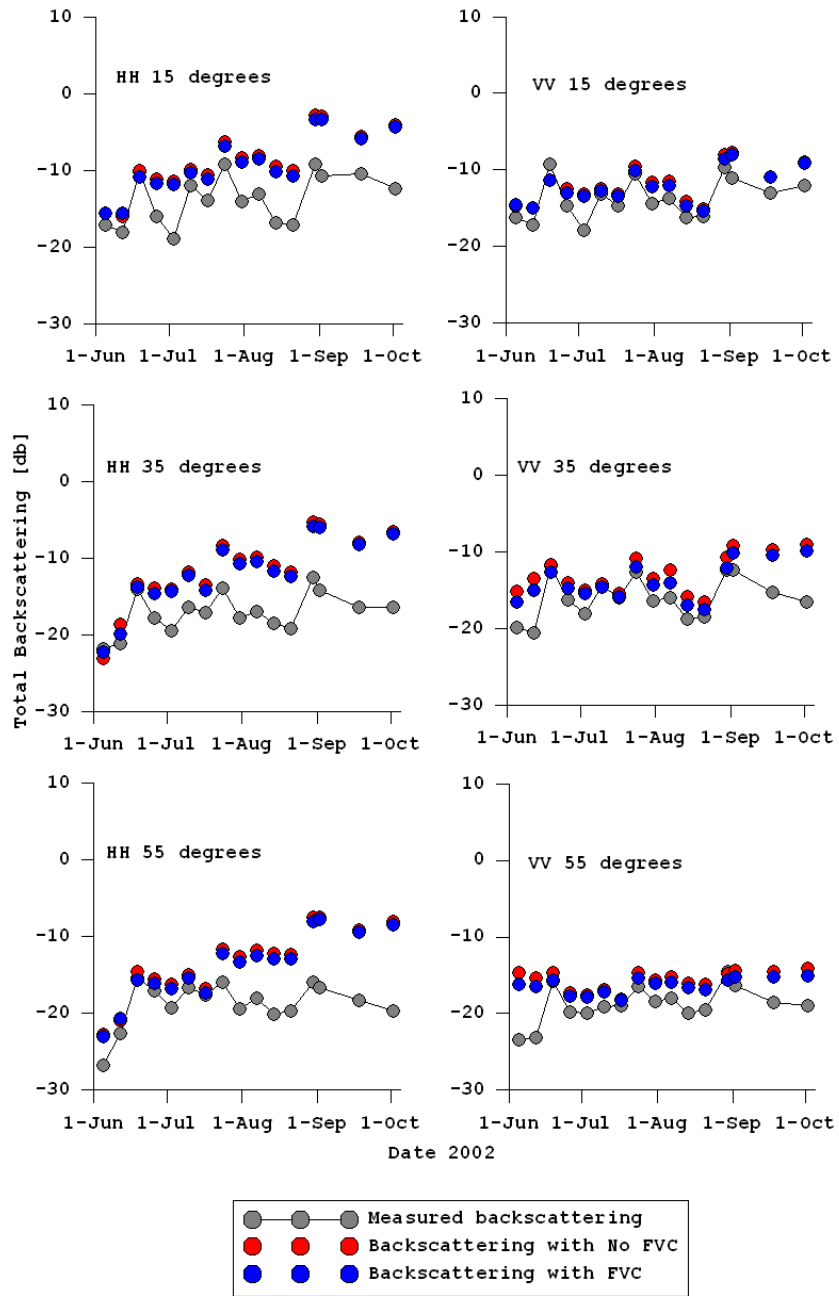


Figure (6-6) Effect of FVC on Tor Vergata model

7. COMPARING THE SCATTERING COMPONENTS

Tor Vergata model is capable of producing the total backscattering and its components. It allows identification of the different scattering sources within the canopy. These components are soil scattering, vegetation-soil scattering and surface scattering attenuated by vegetation as mentioned in section 3.1 and illustrated in Figure (3-1). Analysis for these scattering components helps to understand which component dominates the backscattering throughout various parts of the growth cycle.

In chapter (5) Tor Vergata model simulation with the four soil and vegetation dielectric models, vegetation geometry effect and fraction vegetation cover effect were discussed. In addition, sources of uncertainty in the simulated total backscattering were evaluated. However, the scattering components need to be evaluated.

According to results in chapter (6), Mironov and Matzler dielectric models shows the lowest differences between simulated and measured backscattering. Besides, the sensitivity of Tor Vergata model towards stem orientation rather than leaf orientation especially at maximum stem angle of 15 degrees. Finally, considering the fraction vegetation cover gives closer simulated values to the measured ones.

In the sections below the three scattering components (i.e. surface, vegetation and surface-vegetation) illustrated in Figure (3-1) is evaluated. Tor Vergata model was run with Mironov's soil permittivity model and Matzler's vegetation dielectric model for the following three cases,

1. **Scenario 1:** Applying standard Tor Vergata model (stem max angle =5 degrees and leaf max angle = 85 degrees) with field measurements as an input.
2. **Scenario 2:** Applying the beta version of Tor Vergata model with max stem = 15 degrees and Max leaf =85 degrees for closed canopies together with field measurements.
3. **Scenario 3:** Applying the new version of Tor Vergata model for open canopies with max stem = 15 degrees and Max leaf angle =85 degrees together with field measurements.

7.1. Surface scattering

Figure (7-1) shows the surface scattering component. The surface component is almost the same in case of standard Tor Vergata model and using maximum stem angle of 15 degrees with differences in average 0.5 to 1 dB at both polarizations and at all incidence angles. However, surface scattering component is most affected in case of including the fraction vegetation cover especially at VV polarization. HH polarization shows almost no differences in the surface component in the three cases at all incidence angles at all growth stages.

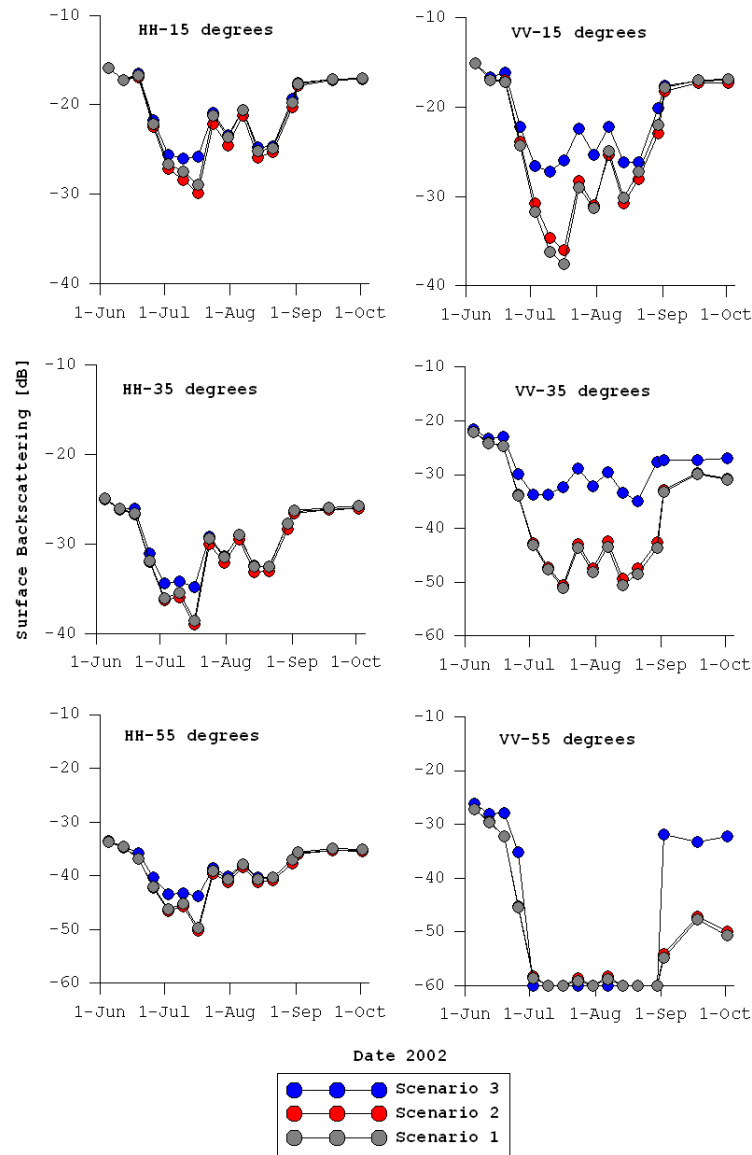


Figure (7-1) Surface scattering component

At initial growth stage in first three week at all incidence angles at VV-polarization, surface component is almost the same for the three cases of simulations as the surface was not covered with corn plant elements yet. Near peak biomass the surface component in case of including the FVC differs significantly from the other two cases with value ranges up to 3 dB as the corn plant leaves and stem getting larger and affects the microwave reflected back to the sensor. However, at 55 degrees the Tor Vergata model fails to simulate the surface component during peak biomass because the attenuation is blocking surface

contribution. Near senescence, the higher incidence angle the difference appears more between the FVC case and the other two cases.

7.2. Vegetation scattering

Figure (7-2) shows the vegetation scattering component shows the same temporal variation with the same values at all incidence angles for both HH & VV polarizations. During the initial growth stage, the vegetation scattering increases steeply with sudden jump in backscattering value ranges up to 5 dB.

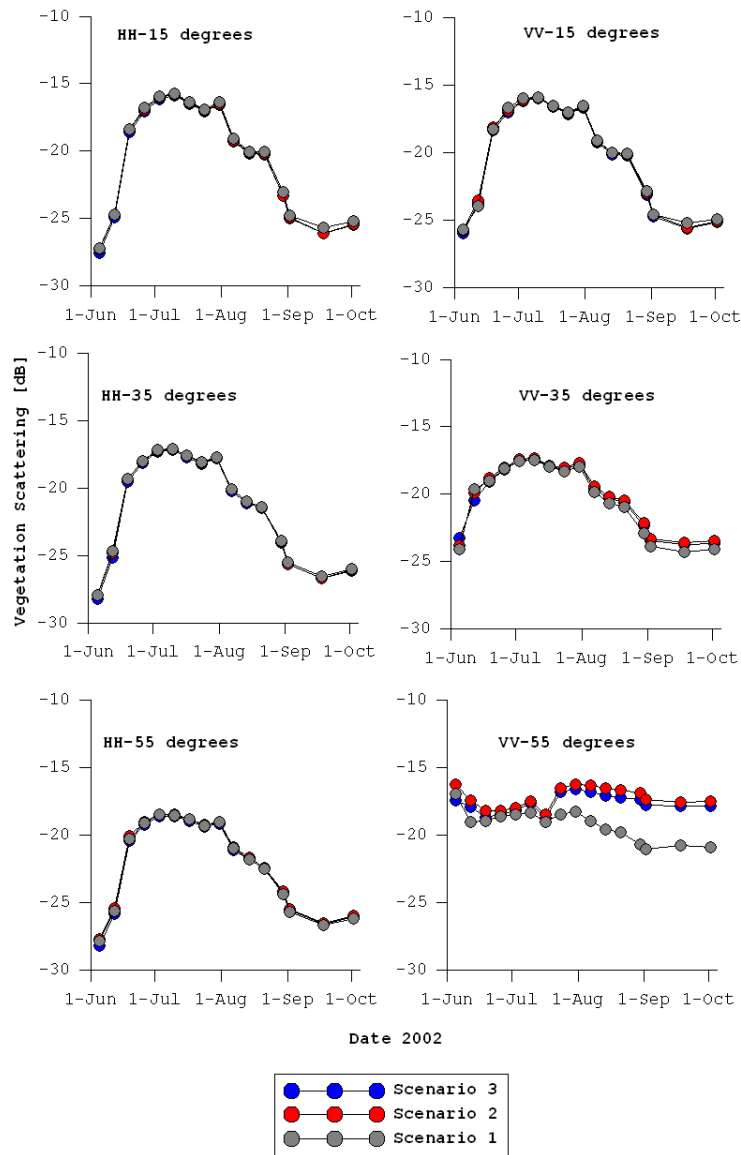


Figure (7-2) Vegetation scattering component

However, near peak biomass the vegetation scattering decreases gradually, but near senescence it decreases with differences from week to another with range of 1 dB. In addition, at VV polarization with incidence angle of 55 degrees shows small differences in vegetation backscattering through the whole growth cycle.

7.3. Vegetation-Surface scattering

Figure (7-3) shows the vegetation–surface scattering component. The new version of Tor Vergata model that includes the effect of fraction vegetation cover shows the lowest scattering hat causes lowering to the total backscattering closer to the measured ones. However, differences in backscattering between the three cases of simulations at all incidence angles at both polarizations are within 2 dB. Increasing stem angle lowers the vegetation-surface component.

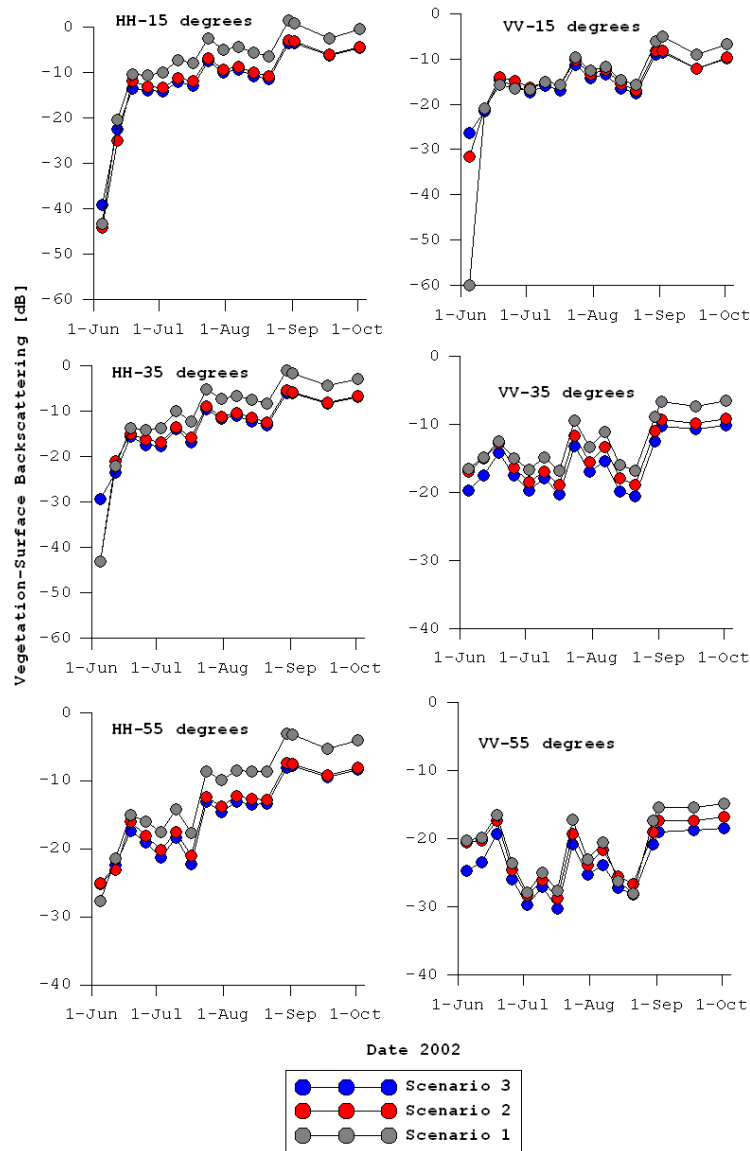


Figure (7-3) Vegetation-Surface scattering

According to previous analysis to different scattering components it is observed that surface and vegetation-surface components are more affected by changes in stem angle and including the FVC. However, near peak biomass the surface scattering component is more affected by including the FVC effect at VV polarization. The vegetation-surface scattering component dominates the scattering from corn canopy through the whole growth cycle.

8. SUMMARY AND CONCLUSIONS

Evaluating the effect of canopy structure and plant water content on microwave data is important to a basic understanding of energy interaction within a vegetation canopy. This research has shown the results of an evaluation study about ability of discrete medium scattering Tor Vergata model to simulate active microwave signatures through corn growth. To meet the objective of this study several research questions needed to be answered. This is done by carrying out simulations of microwave backscattering and comparison with observational data collected over a corn field at L-Band, at three incidence angles and at HH & VV polarizations.

Can discrete medium vegetation scattering model be used to model active microwave observations?

The simulations have shown that the Tor Vergata model is capable of reproducing the backscattering with the same temporal variation as collected in field. However, Tor Vergata model tends to overestimate the measurements. Simulated VV shows more sensitivity to σ^0 at higher angles, whereas several configurations present lower RMSD than HH polarization. At initial growth stage, simulated HH σ^0 have almost the same values as measured ones. Near to peak biomass the simulated VV σ^0 agree very well with measurements at all three incidence angle. Near senescence biomass discrepancies increase between measured and simulated σ^0 at both polarizations. This can explained because at this growth stage the LAI was not measured and assumed the same for the last three weeks.

What is the impact of the employed soil and vegetation dielectric model on the simulated backscatter?

On the other hand, dielectric models play an important role in discrete scattering model through physical and geometrical properties of soil and vegetation. However, uncertainties in the dielectric model affect the simulated backscattering within Tor Vergata model. Four dielectric model combinations were used in this study to evaluate their impact on the simulated σ^0 . Matzler (1994) vegetation model with Mironov (2009) soil model, estimates total backscattering from vegetated covered surface better than other model combinations especially at VV polarization for higher incidence angles.

That is due to the explicit distinction between the electromagnetic properties of bound and free water in Mironov's model which is not considered in Dobson model. In addition, Ulaby & El-Rayes assumed that most of the water in vegetation is in bound form when water content is low and in free form when the water content is high. This assumption produces an error in the predicted dielectric constant for fresh leaves. However, Matzler shows that bound-water effects would have to be considered for dryer leaf material showing lower error of prediction in the dielectric constant

How does the vegetation geometry (e.g. orientation of stems and leaves) affect the simulated backscatter?

Another source of uncertainty within these Tor Vergata model simulations is the orientation of scatterers (e.g. stem and leaves). To investigate this sensitivity of the simulated backscatter, the Tor Vergata model was run using several ranges of leaves and stem inclination angles. These simulations were performed using Matzler's (1994) vegetation permittivity model together with Mironov (2009) soil permittivity model. Tor Vergata model shows no sensitivity to variations in leaf orientations. However, stem angles affect the simulated backscattering within the Tor Vergata model. The larger maximum stem angle the lower and better simulated σ^0 values by Tor Vergata model.

How does the Fraction Vegetation Cover (e.g. orientation of stems and leaves) affect the simulated backscatter?

Discrete medium scattering models considered the soil to be fully covered by vegetation. However, it is often not the case. The vegetation is not fully covering the soil surface. Fraction vegetation cover (FVC) to be given as inputs to the Tor Vergata model, have been related to leaf area index (LAI) by an empirical relationship (Choudhury, 1987). Including the FVC lowers the total backscattering and brings it closer to the measured ones giving better estimates for the simulated backscattering. Especially, VV polarization at all incidence angles the simulated backscatter gets closer to measured backscattering with differences up to 2 dB.

Which scattering component dominates the backscattering throughout various parts of the growth cycle?

Based on analysis for different scattering components it is observed that surface and vegetation-surface components are more affected by changes in stem angle and including the FVC. However, near peak biomass the surface scattering component is more affected by including the FVC effect at VV polarization. The vegetation-surface scattering component dominates the scattering from corn canopy through the whole growth cycle.

LIST OF REFERENCES

- Attema, E. P. W. (1978). Vegetation modeled as a water cloud. *In: Radio science, 13(1978)2, pp. 357-364.*
- Bindlish, R., & Barros, A. P. (2002). Subpixel variability of remotely sensed soil moisture: an inter-comparison study of SAR and ESTAR. *Geoscience and Remote Sensing, IEEE Transactions on, 40(2), 326-337.*
- Bindlish, R., Jackson, T. J., Wood, E., Gao, H., Starks, P., Bosch, D., et al. (2003). Soil moisture estimates from TRMM Microwave Imager observations over the Southern United States. *Remote Sensing of Environment, 85(4), 507-515.*
- Birchak, J. R., Gardner, C. G., Hipp, J. E., & Victor, J. M. (1974). High dielectric constant microwave probes for sensing soil moisture. *Proceedings of the Ieee, 62(1), 93-98.*
- Bracaglia, M., Ferrazzoli, P., & Guerriero, L. (1995). A fully polarimetric multiple scattering model for crops. *Remote Sensing of Environment, 54(3), 170-179.*
- Chauhan, N. S. (1997). Soil moisture estimation under a vegetation cover: Combined active passive microwave remote sensing approach. *International Journal of Remote Sensing, 18(5), 1079 - 1097.*
- Chauhan, N. S., Le Vine, D. M., & Lang, R. H. (1994). Discrete scatter model for microwave radar and radiometer response to corn: comparison of theory and data. *Geoscience and Remote Sensing, IEEE Transactions on, 32(2), 416-426.*
- Choudhury, B. J. (1987). Relationships between vegetation indices, radiation absorption, and net photosynthesis evaluated by a sensitivity analysis. *Remote Sensing of Environment, 22(2), 209-233.*
- Cookmartin, G., Saich, P., Quegan, S., Cordey, R., Burgess-Allen, P., & Sowter, A. (2000). Modeling microwave interactions with crops and comparison with ERS-2 SAR observations. *Geoscience and Remote Sensing, IEEE Transactions on, 38(2), 658-670.*
- Davidson, M. W. J., Thuy Le, T., Mattia, F., Satalino, C., Manninen, T., & Borgeaud, M. (2000). On the characterization of agricultural soil roughness for radar remote sensing studies. *Geoscience and Remote Sensing, IEEE Transactions on, 38(2), 630-640.*
- Della Vecchia, A., Ferrazzoli, P., Guerriero, L., Blaes, X., Defourny, P., Dente, L., et al. (2006). Influence of geometrical factors on crop backscattering at C-band. *Geoscience and Remote Sensing, IEEE Transactions on, 44(4), 778-790.*
- Della Vecchia, A., Ferrazzoli, P., Guerriero, L., Ninivaggi, L., Strozzi, T., & Wegmuller, U. (2008). Observing and Modeling Multifrequency Scattering of Maize During the Whole Growth Cycle. *Geoscience and Remote Sensing, IEEE Transactions on, 46(11), 3709-3718.*
- Dobson, M. C., Ulaby, F. T., Hallikainen, M. T., & El-Rayes, M. A. (1985). Microwave Dielectric Behavior of Wet Soil-Part II: Dielectric Mixing Models. *Geoscience and Remote Sensing, IEEE Transactions on, GE-23(1), 35-46.*
- El-Rayes, M. A., & Ulaby, F. T. (1987). Microwave Dielectric Spectrum of Vegetation-Part I: Experimental Observations. *Geoscience and Remote Sensing, IEEE Transactions on, GE-25(5), 541-549.*
- Entekhabi, D., Njoku, E., & O'Neill, P. (2009, 4-8 May 2009). *The Soil Moisture Active and Passive Mission (SMAP): Science and applications.* Paper presented at the Radar Conference, 2009 IEEE.
- Eom, H. J., & Fung, A. K. (1984). A scatter model for vegetation up to Ku-band. *Remote Sensing of Environment, 15(3), 185-200.*
- Famiglietti, J. S., Rudnicki, J. W., & Rodell, M. (1998). Variability in surface moisture content along a hillslope transect: Rattlesnake Hill, Texas. *Journal of Hydrology, 210(1-4), 259-281.*
- Fung, A. K. (1994). *Microwave scattering and emission models and their applications.* Boston etc.: Artech House.
- Fung, A. K., Li, Z., & Chen, K. S. (1992). Backscattering from a randomly rough dielectric surface. *Geoscience and Remote Sensing, IEEE Transactions on, 30(2), 356-369.*
- Hallikainen, M. T., Ulaby, F. T., Dobson, M. C., El-Rayes, M. A., & Lil-Kun, W. (1985). Microwave Dielectric Behavior of Wet Soil-Part 1: Empirical Models and Experimental Observations. *Geoscience and Remote Sensing, IEEE Transactions on, GE-23(1), 25-34.*
- Joseph, A. T., Van der Velde, R., O'Neill, P. E., Lang, R., & Gish, T. (2010). Effects of corn on C- and L-band radar backscatter: A correction method for soil moisture retrieval. *Remote Sensing of Environment.*
- Joseph, A. T., van der Velde, R., O'Neill, P. E., Lang, R. H., & Gish, T. (2008). Soil Moisture Retrieval During a Corn Growth Cycle Using L-Band (1.6 GHz) Radar Observations. *Geoscience and Remote Sensing, IEEE Transactions on, 46(8), 2365-2374.*

- Karam, M. A., & Fung, A. K. (1988). ELECTROMAGNETIC SCATTERING FROM A LAYER OF FINITE LENGTH, RANDOMLY ORIENTED, DIELECTRIC, CIRCULAR-CYLINDERS OVER A ROUGH INTERFACE WITH APPLICATION TO VEGETATION. *International Journal of Remote Sensing*, 9(6), 1109-1134.
- Karam, M. A., Fung, A. K., Lang, R. H., & Chauhan, N. S. (1992). A microwave scattering model for layered vegetation. *Geoscience and Remote Sensing, IEEE Transactions on*, 30(4), 767-784.
- Kerr, Y. H., Waldteufel, P., Wigneron, J. P., Delwart, S., Cabot, F., Boutin, J., et al. (2010). The SMOS Mission: New Tool for Monitoring Key Elements of the Global Water Cycle. *Proceedings of the IEEE*, 98(5), 666-687.
- Kerr, Y. H., Waldteufel, P., Wigneron, J. P., Martinuzzi, J., Font, J., & Berger, M. (2001). Soil moisture retrieval from space: the Soil Moisture and Ocean Salinity (SMOS) mission. *Geoscience and Remote Sensing, IEEE Transactions on*, 39(8), 1729-1735.
- Lang, R. H., & Sidhu, J. S. (1983). Electromagnetic Backscattering from a Layer of Vegetation: A Discrete Approach. *Geoscience and Remote Sensing, IEEE Transactions on, GE-21(1)*, 62-71.
- LeVine, D. M., Meneghini, R., Lang, R. H., & Seker, S. S. (1983). Scattering from arbitrarily oriented dielectric disks in the physical optics regime. *J. Opt. Soc. Am.*, 73(10), 1255-1262.
- Macelloni, G., Paloscia, S., Pampaloni, P., Marliani, F., & Gai, M. (2001). The relationship between the backscattering coefficient and the biomass of narrow and broad leaf crops. *Geoscience and Remote Sensing, IEEE Transactions on*, 39(4), 873-884.
- Maity, S., Patnaik, C., Chakraborty, M., & Panigrahy, S. (2004). Analysis of temporal backscattering of cotton crops using a semiempirical model. *Geoscience and Remote Sensing, IEEE Transactions on*, 42(3), 577-587.
- Matzler, C. (1994). Microwave (1-100 GHz) dielectric model of leaves. *Geoscience and Remote Sensing, IEEE Transactions on*, 32(4), 947-949.
- Mironov, V. L., Dobson, M. C., Kaupp, V. H., Komarov, S. A., & Kleshchenko, V. N. (2002, 24-28 June 2002). *Generalized refractive mixing dielectric model for moist soils*. Paper presented at the Geoscience and Remote Sensing Symposium, 2002. IGARSS '02. 2002 IEEE International.
- Mironov, V. L., Kosolapova, L. G., & Fomin, S. V. (2009). Physically and Mineralogically Based Spectroscopic Dielectric Model for Moist Soils. *Geoscience and Remote Sensing, IEEE Transactions on*, 47(7), 2059-2070.
- Narayan, U., Lakshmi, V., & Njoku, E. G. (2004). Retrieval of soil moisture from passive and active L/S band sensor (PALS) observations during the Soil Moisture Experiment in 2002 (SMEX02). *Remote Sensing of Environment*, 92(4), 483-496.
- Njoku, E. G., Wilson, W. J., Yueh, S. H., Dinardo, S. J., Li, F. K., Jackson, T. J., et al. (2002). Observations of soil moisture using a passive and active low-frequency microwave airborne sensor during SGP99. *Geoscience and Remote Sensing, IEEE Transactions on*, 40(12), 2659-2673.
- Njoku, E. G., Wilson, W. J., Yueh, S. H., & Rahmat-Samii, Y. (2000). A large-antenna microwave radiometer-scatterometer concept for ocean salinity and soil moisture sensing. *Geoscience and Remote Sensing, IEEE Transactions on*, 38(6), 2645-2655.
- O'Neill, P. E., Jackson, T. J., Blanchard, B. J., Wang, J. R., & Gould, W. I. (1984). Effects of corn stalk orientation and water content on passive microwave sensing of soil moisture. [doi: DOI: 10.1016/0034-4257(84)90027-0]. *Remote Sensing of Environment*, 16(1), 55-67.
- Owe, M., de Jeu, R., & Walker, J. (2001). A methodology for surface soil moisture and vegetation optical depth retrieval using the microwave polarization difference index. *Geoscience and Remote Sensing, IEEE Transactions on*, 39(8), 1643-1654.
- Schiffer, R., & Thielheim, K. O. (1979). Light scattering by dielectric needles and disks. *Journal of Applied Physics*, 50(4), 2476-2483.
- Schmugge, T. J. (1983). Remote Sensing of Soil Moisture: Recent Advances. *Geoscience and Remote Sensing, IEEE Transactions on, GE-21(3)*, 336-344.
- Schmugge, T. J., Kustas, W. P., Ritchie, J. C., Jackson, T. J., & Rango, A. (2002). Remote sensing in hydrology. *Advances in Water Resources*, 25(8-12), 1367-1385.
- Seker, S. S., & Schneider, A. (1988). Electromagnetic scattering from a dielectric cylinder of finite length. *Antennas and Propagation, IEEE Transactions on*, 36(2), 303-307.
- Toure, A., Thomson, K. P. B., Edwards, G., Brown, R. J., & Brisco, B. G. (1994). Adaptation of the MIMICS backscattering model to the agricultural context-wheat and canola at L and C bands. *Geoscience and Remote Sensing, IEEE Transactions on*, 32(1), 47-61.
- Ulaby, F. (1980). Vegetation clutter model. *Antennas and Propagation, IEEE Transactions on*, 28(4), 538-545.

- Ulaby, F., & Batlivala, P. (1976). Diurnal variations of radar backscatter from a vegetation canopy. *Antennas and Propagation, IEEE Transactions on*, 24(1), 11-17.
- Ulaby, F., & Bush, T. (1976). Corn growth as monitored by radar. *Antennas and Propagation, IEEE Transactions on*, 24(6), 819-828.
- Ulaby, F. T., Bradley, G. A., & Dobson, M. C. (1979). Microwave Backscatter Dependence on Surface Roughness, Soil Moisture, and Soil Texture: Part II-Vegetation-Covered Soil. *Geoscience Electronics, IEEE Transactions on*, 17(2), 33-40.
- Ulaby, F. T., & El-Rayes, M. A. (1987). Microwave Dielectric Spectrum of Vegetation - Part II: Dual-Dispersion Model. *Geoscience and Remote Sensing, IEEE Transactions on*, GE-25(5), 550-557.
- Ulaby, F. T., McDonald, K., Sarabandi, K., & Dobson, M. C. (1988). *Michigan Microwave Canopy Scattering Models (MIMICS)*. Paper presented at the Geoscience and Remote Sensing Symposium, 1988. IGARSS '88. Remote Sensing: Moving Toward the 21st Century., International.
- Ulaby, F. T., Moore, R. K., & Fung, A. K. (1981). *Microwave remote sensing : active and passive : Vol. III from theory to applications*. Reading etc.: Addison-Wesley.
- Vine, D. M. L., Pellerano, F., Lagerloef, G. S. E., Yueh, S., & Colomb, R. (2006, 2006). *Aquarius: A Mission to Monitor Sea Surface Salinity from Space*. Paper presented at the IEEE MicroRad, 2006.
- Wagner, W., Blochl, G., Pampaloni, P., Calvet, J. C., Bizzarri, B., Wigneron, J. P., et al. (2007). Operational readiness of microwave remote sensing of soil moisture for hydrologic applications. *Nordic Hydrology*, 38(1), 1-20.
- Wen, J., Su, Z. B., & Ma, Y. M. (2003). Determination of land surface temperature and soil moisture from Tropical Rainfall Measuring Mission/Microwave Imager remote sensing data. *Journal of Geophysical Research-Atmospheres*, 108(D2).
- Wigneron, J. P., Ferrazzoli, P., Calvet, J. C., & Bertuzzi, P. (1999). A parametric study on passive and active microwave observations over a soybean crop. *Geoscience and Remote Sensing, IEEE Transactions on*, 37(6), 2728-2733.
- Wilson, W. J., Yueh, S. H., Dinardo, S. J., Chazanoff, S. L., Kitiyakara, A., Li, F. K., et al. (2001). Passive active L- and S-band (PALS) microwave sensor for ocean salinity and soil moisture measurements. *Geoscience and Remote Sensing, IEEE Transactions on*, 39(5), 1039-1048.
- Wood, E. F., Lin, D. S., Mancini, M., Thongs, D., Troch, P. A., Jackson, T. J., et al. (1993). Intercomparisons between passive and active microwave remote sensing, and hydrological modeling for soil moisture. *Advances in Space Research*, 13(5), 167-176.